VTT PUBLICATIONS 280

Microstructural degradation of boiler tube steels under long term exposure to high temperature

Jorma Salonen & Pertti Auerkari

VTT Manufacturing Technology

TECHNICAL RESEARCH CENTRE OF FINLAND
ESPOO 1996

ISBN 951-38-4938-4
ISSN 1235-0621

JULKAISIJA – UTGIVARE – PUBLISHER

Valtion teknillinen tutkimuskeskus (VTT), Vuorimiehentie 5, PL 2000, 02044 VTT
puh. vaihde (09) 4561, faksi (09) 456 4374

Statens tekniska forskningscentral (VTT), Bergsmansvägen 5, PB 2000, 02044 VTT
tel. växel (09) 4561, fax (09) 456 4374

Technical Research Centre of Finland (VTT), Vuorimiehentie 5, P.O.Box 2000, FIN–02044 VTT, Finland
phone internat. + 358 9 4561, fax + 358 9 456 4374

VTT Valmistustekniikka, Materiaalien valmistustekniikka, Metallimiehenkuja 2–6, PL 1703, 02044 VTT
puh. vaihde (09) 4561, faksi (09) 463 118
VTT Tillverkningsteknik, Materialteknik, Metallmansgränden 2–6, PB 1703, 02044 VTT
tel. växel (09) 4561, fax (09) 463 118
VTT Manufacturing Technology, Materials Technology, Metallimiehenkuja 2–6, P.O.Box 1703,
FIN–02044 VTT, Finland
phone internat. + 358 9 4561, fax + 358 9 463 118

VTT Valmistustekniikka, Käyttötekniikka, Kemistintie 3, PL 1704, 02044 VTT
puh. vaihde (09) 4561, faksi (09) 456 7002
VTT Tillverkningsteknik, Driftsäkerhetsteknik, Kemistvägen 3, PB 1704, 02044 VTT
tel. växel (09) 4561, fax (09) 456 7002
VTT Manufacturing Technology, Operational Reliability, Kemistintie 3, P.O.Box 1704,
FIN–02044 VTT, Finland
phone internat. + 358 9 4561, fax + 358 9 456 7002

VTT OFFSETPAINO, ESPOO 1996

Salonen, Jorma & Auerkari, Pertti. Microstructural degradation of boiler tube steels under long term exposure to high temperature. Espoo 1996, Technical Research Centre of Finland, VTT Publications 280. 20 p. + app. 47 p.

UCD 624.014.27:620.1:620.187
Keywords microstructure, hardness, tests degradation, thermal degradation, boilers, tubes, steels, temperature, microscopy, photomicrographs, classifying

ABSTRACT

Thermal microstructural degradation was investigated by isothermal annealing of samples from boiler tube steels St 35.8, 15 Mo 3, 13 CrMo 44, 10 CrMo 9 10 and X20 CrMoV 12 1 in the temperature range 600 - 780°C for up to 2 000 h. Optical and scanning electron microscopy and hardness testing were used for characterising the microstructural changes and their time-temperature dependence. The results suggest a simple and consistent time-temperature dependence for all investigated materials, expected to apply also to long term service beyond the annealing time range of the present work. This would allow assessment of the in-service thermal exposure from the observed microstructure. A collection of micrographs has been prepared for this purpose, to aid in classifying and evaluating the observed microstructural state in terms of isothermal exposure to high temperature.

PREFACE

This work is a compilation from selected projects originally performed and financed mainly through an internal R&D effort of VTT Manufacturing Technology in 1992 - 1995. The tube materials used in the research were kindly donated by Helsinki Energy.

CONTENTS

1 INTRODUCTION

Properties such as strength of steels used at high temperatures are strongly dependent on microstructure. However, useful initial microstructures are not stable in service conditions but change gradually at a temperature-dependent rate through processes of thermal degradation. Many of these processes of importance consist of changes in the carbide structure of the steels. Basically, in unalloyed or only slightly alloyed ferritic-pearlitic steels the most obvious degradation process is that of the cementite (Fe_3C), which will change its appearance rather than composition. In low-alloy steels also considerable compositional changes in the carbides will occur, so that the initial mixture of cementite and M_2C type carbides will evolve to a more complex set of carbides including M_7C_3, $M_{23}C_6$ and eventually M_6C. In high-alloy steels such as 9 to 12% chromium steels, particularly $M_{23}C_6$ type carbides are present early and remain in the structure, showing gradual coarsening during high temperature exposure. In addition, in steels containing vanadium, such as the low alloy type 14 MoV 63 or the high alloy type X20 CrMoV 12 1, very small vanadium carbonitrides provide an essential part of the mechanical strength but are only visible under transmission electron microscopy.

The initial microstructure can vary considerably in some steels depending on the details of the heat treatment, and particularly the rate of cooling in it. Because the austenitising or tempering temperatures vary less and because of fairly extensive standardisation of the boiler steels, it is in practice the effective section thickness that largely determines the initial range of microstructures. Particularly for relatively small wall thicknesses like those for boiler tubes, this initial microstructure is nearly constant.

In addition to changes in carbide composition and geometry, other material and temperature dependent microstructural changes occur at high temperature, such as recrystallisation, grain growth, evolution of the dislocation structure and environmentally enhanced changes like oxidation and decarburisation.

The thermal degradation of a particular feature in the microstructure, when limited to a single degradation mechanism or to a narrow range of temperature, is expected to follow general Arrhenius type kinetics with a reaction rate of

$$dV/dt = Ae^{-Q/kT}, \quad (1)$$

where A is a material dependent constant, Q is the apparent activation energy of degradation, k is the Boltzmann constant and T is absolute temperature (K).

This means that for an equal state after such a reaction, the time and temperature required for a change by the reaction to this state show a linear dependence in $1/T$-

log *t* coordinates. To give a numerical value for such a state, i.e. a combination of time and temperature to yield the same microstructure, the Equation 1 can be simplifed to a number of parametric expressions, the commonest one of being is the Larson-Miller parameter

$$P_{LM} = T \times (\log t + C), \quad (2)$$

where T is again absolute temperature (K) and *t* is time (h), and C is a material and reaction dependent constant.

The purpose of this work is to characterise the time-temperature dependence of microstructural degradation in most common boiler steels, applied to a section size typical to boiler tubes. For applications, a compilation of optical micrographs has been created to support the assessment of the thermal history of boiler tubes after prolonged service at high temperatures. All microstructural changes targeted within this work are limited to the range of normal service, i.e. below the austenitising temperatures.

2 MATERIALS AND METHODS

2.1 MATERIALS

The test materials were received as superheater-size tubes of five base materials, St 35.8, 15 Mo 3, 13 CrMo 4 4, 10 Cr Mo 9 10 and X20 CrMoV 12 1 (DIN 17175). All tubes were of as-new commercial grade materials. Table 1 shows the chemical composition and Table 2 the dimensions and mechanical properties of the tube samples.

Table 1. Chemical composition of the test materials (wt-%).

Steel type		**C**	**Si**	**Mn**	**Cr**	**Mo**	**Ni**	**V**
St 35.8	**1)**	0.09	0.21	0.51				
	2)	≤ 0.17	0.10-0.35	0.40-0.80				
15 Mo 3	**1)**	0.17	0.24	0.70		0.27		
	2)	0.12-0.20	0.10 - 0.35	0.40 - 0.80		0.25 - 0.35		
13 CrMo 4 4	**1)**	0.13	0.26	0.56	0.81	0.45		
	2)	0.10-0.18	0.10-0.35	0.40-0.60	0.70-1.1	0.45-0.65		
10 CrMo 9 10	**1)**	0.10	0.21	0.50	2.18	1.02		
	2)	0.08-0.15	<0.50	0.40-0.80	2.0-2.5	0.90-1.20		
X20CrMoV121	**1)**	0.19	0.25	0.61	12.00	0.91	0.65	0.28
	2)	0.17-0.23	≤ 0.50	≤ 1.00	10-12.5	0.80-1.20	0.3-0.8	0.2-0.35

1) According to manufacturer's certificate

2) Required by DIN 17175.

Table 2. Dimensions and initial mechanical properties of the tube samples.

Steel type		Dimensions (mm)	Rm (N/mm^2)	ReL (N/mm^2)	A5 (%)
St 35.8	**1)**	ø 38.0 x 4.0	454 - 456	340 - 344	32.6 - 33
	2)		360 - 480	≥ 235	≥ 25
15 Mo 3	**1)**	ø 57.0 x 5.0	476 - 522	322 - 361	27.5 - 32.4
	2)		450 - 600	≥ 285	≥ 22
13 CrMo 44	**1)**	ø 38.0 x 3.2	457 - 477	331 - 347	30 - 34
	2)		440 - 590	≥ 290	≥ 22
10 CrMo 9 10	**1)**	ø 38.0 x 4.5	513 - 516	420 - 426	28 - 29
	2)		450 - 600	≥ 280	≥ 20
X 20 CrMoV 121	**1)**	ø 38.0 x 4.5	809 - 813	573 - 576	20.0 - 21.1
	2)		690 - 840	≥ 490	≥ 17

1) According to the manufacturer's certificate
2) Required by DIN 17 175.

Steels St 35.8 and 15 Mo 3 are usually delivered in a normalised state, and steels 13 CrMo 4 4, 10 CrMo 9 10 and X20 CrMoV 12 1 in normalised/ quenched and tempered state. For welded products a post-weld heat treatment (PWHT) is possible but not always required for thin boiler tubes up to and including grade 10 CrMo 9 10. Both tempering and PWHT are especially important for the high alloy steel X20 CrMoV 12 1, which becomes fully martensitic after cooling in air from austenitising temperatures. The heat treatment characteristics of the steels are shown in Table 3.

Table 3. Heat treatment characteristics of the test materials.

Steel type	A_1	Austenitising 1)	Temper/PWHT 1)
St 35.8	~725°C	900 - 930°C	- / 520 - 600°C
15 Mo 3	~725°C	910 - 940°C	- / 530 - 620°C
13 CrMo 4 4	~745°C	910 - 940°C	660 - 730 / 600 - 700°C
10 CrMo 9 10	~780°C	900 - 960°C	700 - **750** / 650 - 750°C
X 20 CrMoV 12 1	~800°C	1020 - 1070°C	730 - 780 / 720 - 780°C

1) According to DIN 17 175; in bold when quoted by the manufacturer.

2.2 METHODS

Test samples cut from the boiler tubes were isothermally annealed in air in a laboratory furnace, using a test temperature from the range 600 - 780°C (±3°C) and annealing times between 1 h and 2 000 h. The selected annealing temperature and annealing time combinations are shown in Table 4. The highest testing temperatures required that the specimens be encapsulated in gas-tight stainless steel capsules to avoid excessive oxidation and decarburisation.

Table 4. Annealing times and temperatures for the test materials.

Steel type	Annealing temperature (°C)	Annealing time (h)
St 35.8	600	1-300
	660	1-300
	720	1-100
15 Mo 3	600	1-1000
	660	1-300
	720	1-100
13 CrMo 4 4	600	1-300
	660	1-300
	720	1-100
	740	1-2000
10 CrMo 9 10	600	1-300
	660	1-300
	720	1-300
	740	1-2000
X 20 CrMoV 12 1	600	1-300
	660	1-300
	720	1-1000
	780	1-2000

Cross-sections of annealed samples were studied metallographically with light optical microscopy (LOM), and selected samples also with scanning electron microscopy (SEM). The same cross-sections were used for measuring the Vickers hardness (HV5) of the steel samples.

3 RESULTS AND DISCUSSION

3.1 MICROSTRUCTURAL INVESTIGATION

The microstructures resulting from isothermal annealing are shown as light optical micrographs in Appendix 1 (Figs 1 to 43) and as corresponding scanning electron micrographs in Appendix 2 (Figs 1 to 50).

In steels St 35.8 and 15 Mo 3 microstructural degradation starts as breaking of the pearlite lamellae and gradual globularisation of the initially nearly intact lamellar structure of the pearlite, followed by gradual coarsening of carbides. Details of the initial changes are not discernible with LOM, but the starting point is generally observed as early as with SEM.

In steels 13 CrMo 44 ja 10 CrMo 9 10 the initial microstructure is a ferritic-bainitic structure tempered at a relatively high temperature, inducing some carbide changes already. With LOM the initially discernible degradation appears as lighter bainite regions (compared with the originally relatively dark bainite), showing the lath structure of bainite increasingly clearly. SEM shows that this lighter appearance of bainite is due to coarsening of individual carbides, so that the proportion of relatively flat surface within the bainitic structure increases. The degradation then continues through coarsening of the carbides in bainite (especially along grain boundaries), with gradual coarsening and destruction of the bainitic lath structure.

The initial microstructure of the high-alloy steel X 20 CrMoV 12 1 is martensite, tempered at a high temperature. The initial degradation appears under LOM as coarsening of the lath structure and lightening of the internal structure of the laths, apparently due to coarsening of carbides. With continuing degradation the size of individual carbides finally become discernible under LOM, at first usually on the austenite grain boundaries. Thereafter degradation proceeds as continuous coarsening of the lath structure and carbides.

To evaluate the thermal degradation, the following modified CEGB scale was used for the ferritic-pearlitic steels St 35.8 and 15 Mo 3 (Toft & Marsden 1961; Viswanathan 1989):

A As-new microstructure, ferrite and pearlite
B First signs of disintegration of the pearlite lamellae
C Considerable spherodisation, some lamellar carbides still discernible
D Fully globular carbides, still in the former pearlite regions
E Carbides widely spread, still some indications of the former pearlite regions
F Former pearlite regions no longer discernible, some carbides considerably coarsened
G As F, but grain growth observed in ferrite.

This classification is less well suited to other steels of the present work, because the microstructures are normally not ferritic-pearlitic but either ferritic-bainitic (13 CrMo 4 4 and 10 CrMo 9 10) or martensitic (X 20 CrMoV 12 1). These steels have been tempered during manufacturing at a temperature that has already induced some microstructural changes. Further annealing in testing (or in service) will simply continue these gradual changes towards structural coarsening. For these steels the following scale of evaluating the microstructural degradation was used:

A As-new microstructure of untempered steel
B As-new microstructure of normal tempered steel
C First signs (LOM) of degradation in bainite or martensite
D First discernible (LOM) separate carbides
E Sizeable carbides particularly on grain boundaries, original structure (bainite regions/lath structure) still partially discernible
F Ferrite and carbides, original structure no longer discernible.

Any assessment based solely on the above qualitative definitions is somewhat subjective, including the correspondence of the definitions and the microstructural evaluation of steel samples of the present work. However, to reduce this subjectivity in any subsequent evaluations, the example micrographs of Appendices 1 and 2 can be used as reference.

The results of microstructural investigations are shown in Figures 1 to 5 according to the above classification as time-temperature dependence. It is seen that to produce an equal microstructural degradation, the required time-temperature combinations appear on parallel lines. In addition to carbide changes, graphitisation was observed in 15 Mo3 at 600°C after more than 300 h of annealing.

The results are not corrected for tempering of steels 13 CrMo 4 4, 10 CrMo 9 10 and X 20 CrMoV 12 1, because the details of the original heat treatments are not known and because commercial boiler tubes are likely to be subjected to roughly equivalent tempering.

To assess the value of the LM constant C, as equal microstructures as possible were sought at different annealing time-temperature combinations.

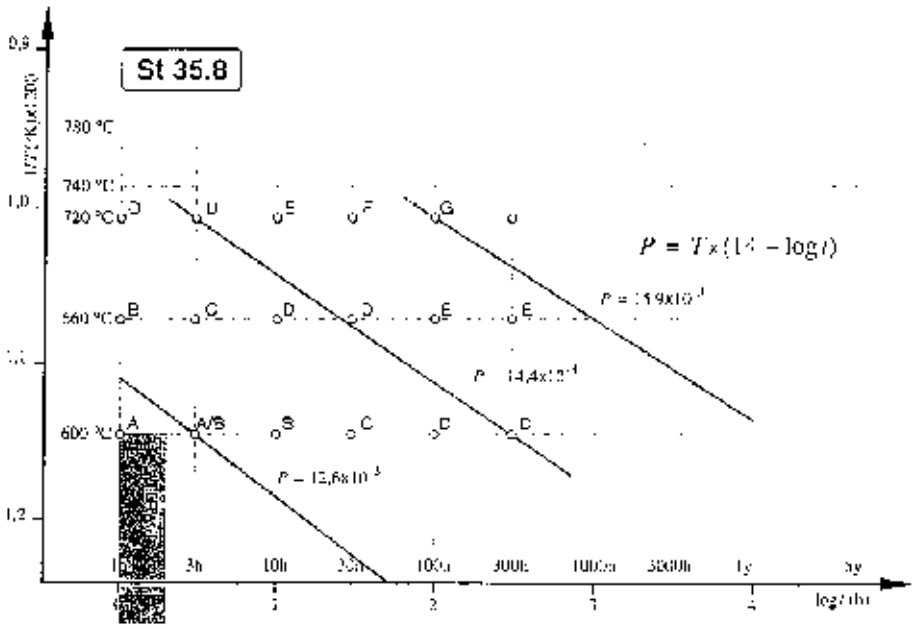

Fig. 1. Time-temperature dependence of microstructural degradation in unalloyed steel St 35.8.

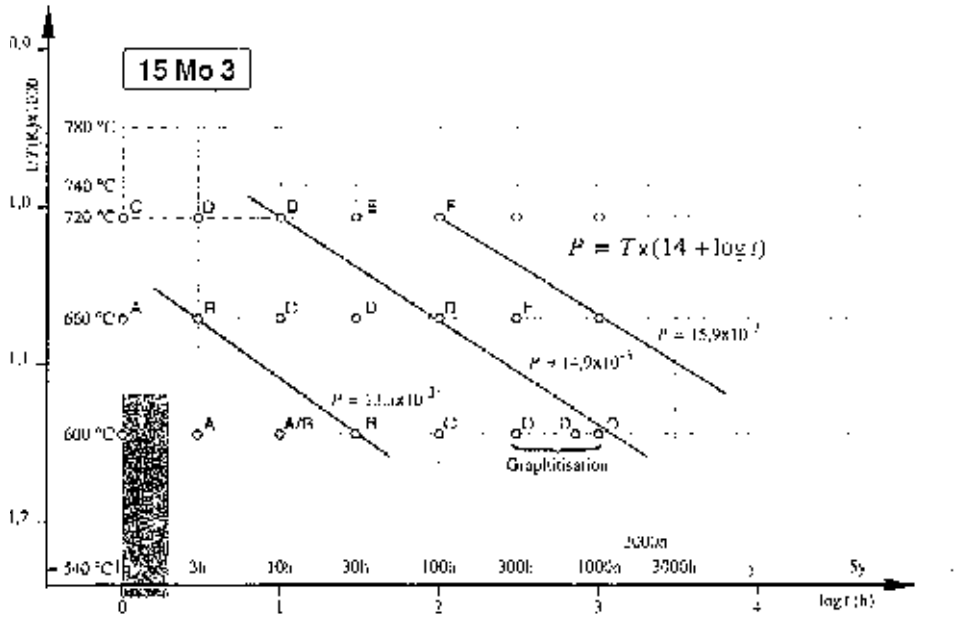

Fig. 2. Time-temperature dependence of microstructural degradation in steel 15 Mo 3.

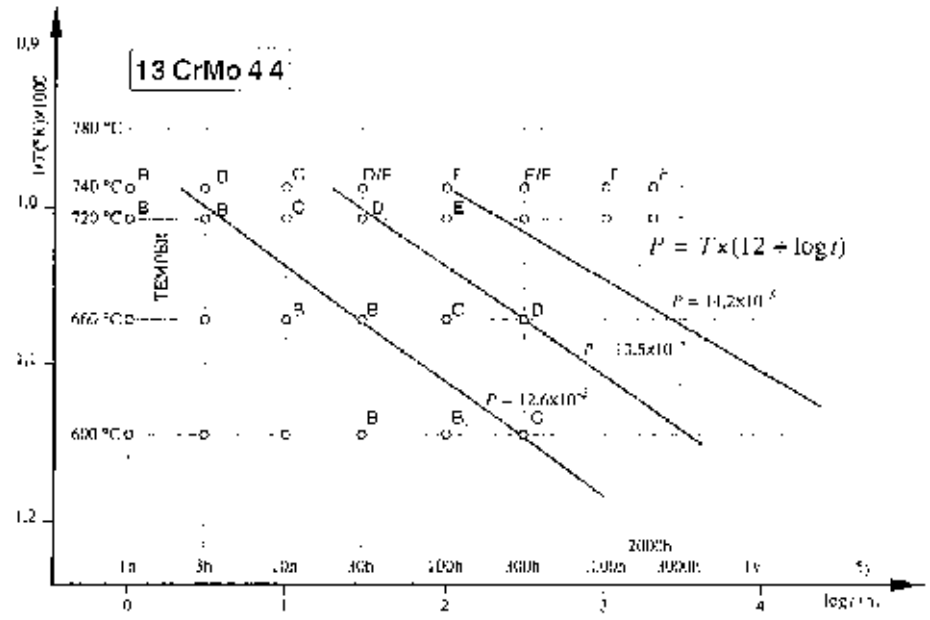

Fig. 3. Time-temperature dependence of isothermal microstructural changes in steel 13 CrMo 4 4.

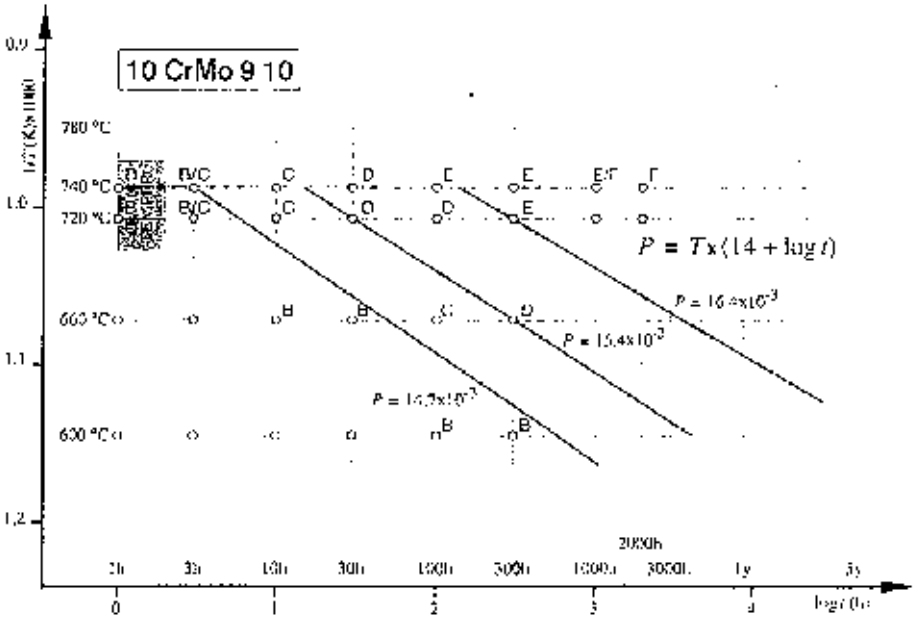

Fig. 4. Time-temperature dependence of isothermal microstructural changes in steel 10 CrMo 9 10.

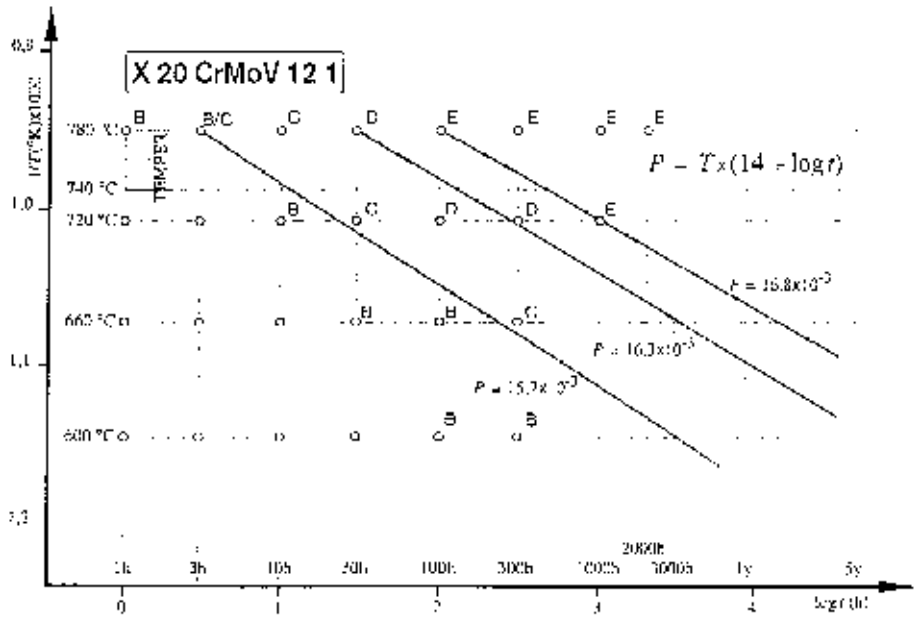

Fig. 5. Time-temperature dependence of isothermal microstructural changes in steel X 20 CrMoV 12 1.

The fitted values (rounded to the nearest integer) of the LM constant are

C = 14 for steels St 35.8, 15 Mo 3, 10 CrMo 9 10 and X20 CrMoV 12 1;
and
C = 12 for steel 13 CrMo 4 4.

The uncertainty in estimating the value of C was smallest for steel types St 35.8 and 15 Mo 3, with a distance between data points of 120°C in temperature and two orders of magnitude in time. For the other materials the corresponding distance was only 60°C in temperature. The range of variation in the value of C was estimated to be about ±2 - 3, and slightly less for the steels St 35.8 and 15 Mo 3. Therefore, within the estimated uncertainty it can be assumed that C = 14 for all steels of this work.

In all cases the value of C has been estimated from lines outside the tempering regions given by DIN 17175 (shown in Figs 1 - 5). This has the effect that the original tempering treatment exerts a negligible influence on the estimated values of C. Figure 6 shows the dependence of the microstructural changes on the value of the isothermal LM parameter for all steel types of the present work.

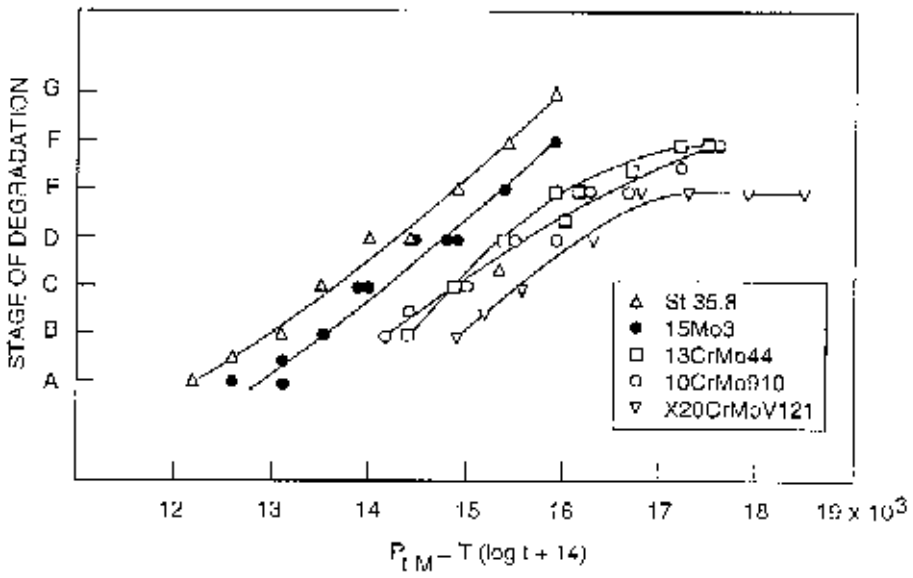

Fig. 6. Thermal degradation as a function of the LM parameter corresponding to isothermal annealing. Note that the degradation scale involves different definitions for ferritic-pearlitic (St 35.8 and 15 Mo 3) and other steels.

The value C = 14 means approximately that an order of magnitude difference in annealing time corresponds to a 60°C difference in temperature. Since for microstructural changes the value of C is clearly less than the common value (C = 20) often assigned to the time-temperature correspondence of creep failure, the kinetics of creep failure and microstructural degradation can be clearly different. However, the common observation that shorter term creep tests correspond to higher values of C than long-term tests approaching service behaviour would suggest that this discrepancy need not to be universal.

3.2 HARDNESS TESTING

The hardness testing results are shown in Figures 7 to 11. Generally the time-temperature combinations to yield equal hardness appear as lines with similar slopes as for microstructural changes in Figures 1 to 5.

Figures 7 to 11 also show the time-temperature limits for lowering the hardness to a level corresponding to the minimum tensile strength according to DIN 17175. These hardness limits have been estimated by assuming linear proportionality between hardness and tensile strength, and multiplying the measured initial hardness by the ratio of minimum strength to initial strength (Table 2).

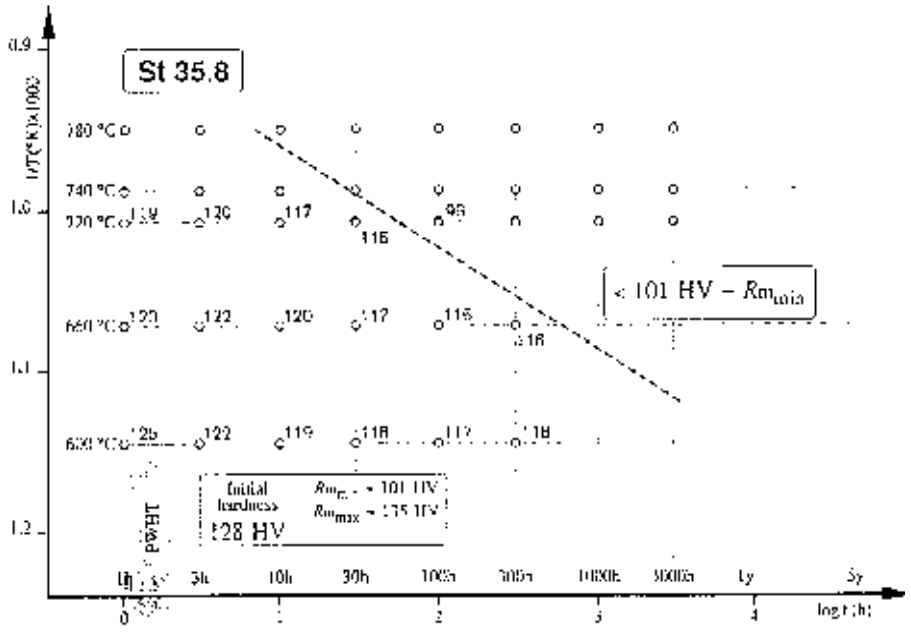

Fig. 7. Time-temperature dependence of hardness changes in steel St 35.8.

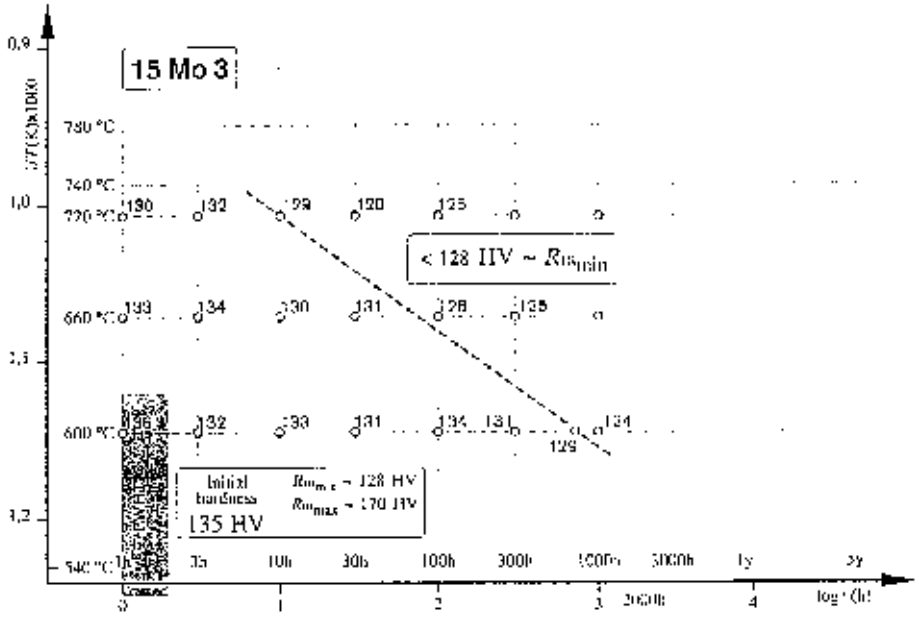

Fig. 8. Time-temperature dependence of hardness changes in steel 15 Mo 3.

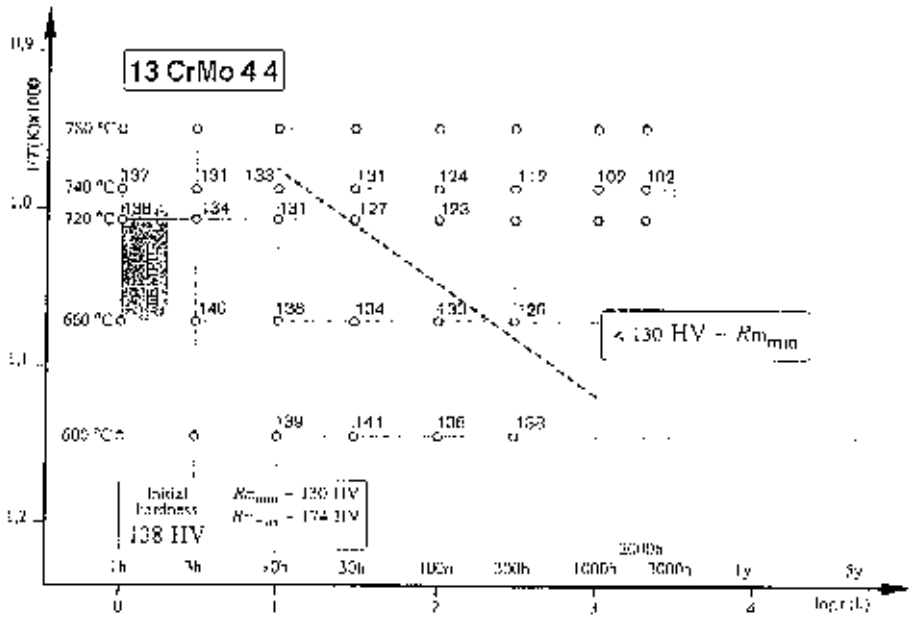

Fig. 9. Time-temperature dependence of isothermal hardness changes in steel 13 CrMo 4 4.

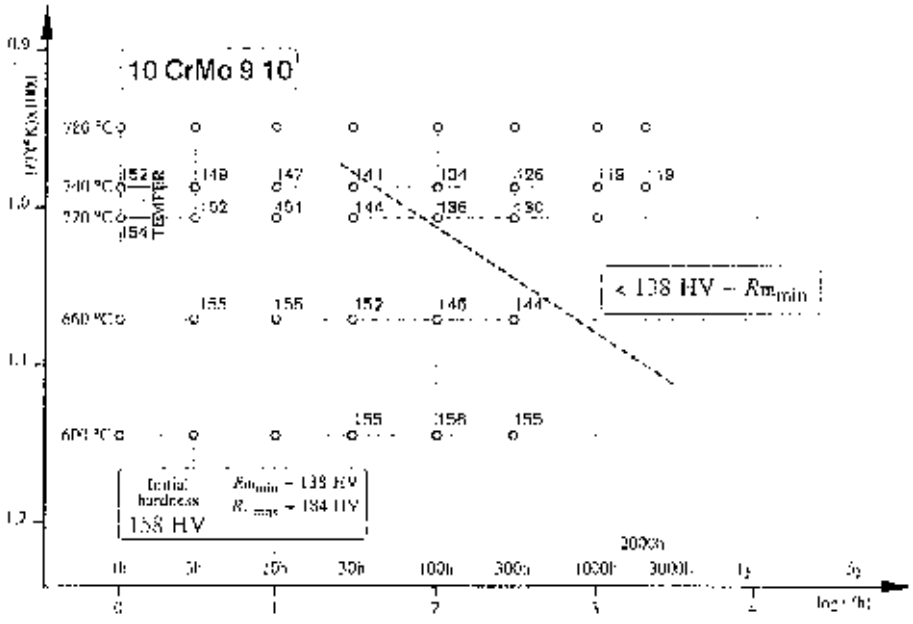

Fig. 10. Time-temperature dependence of hardness changes in steel 10 CrMo 9 10.

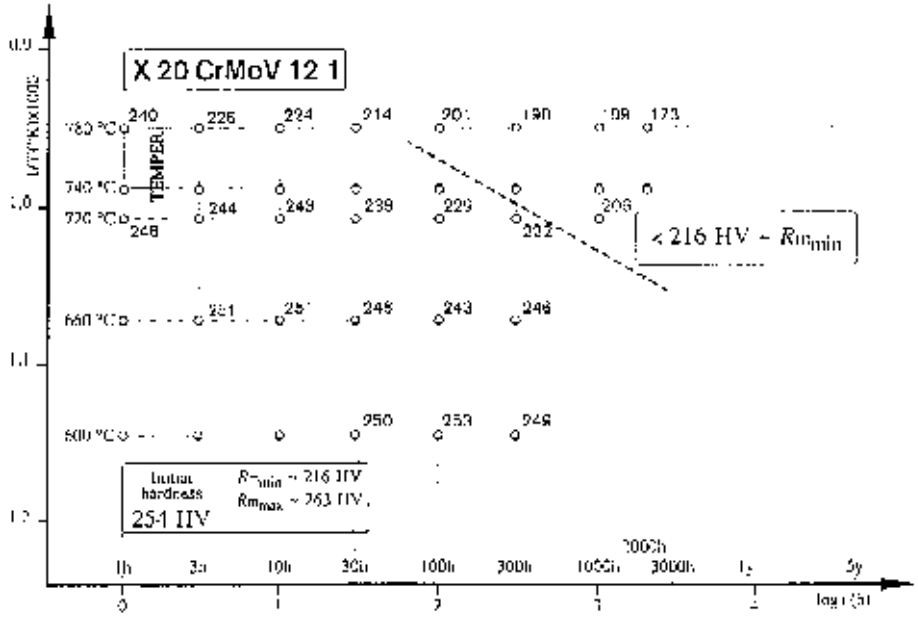

Fig. 11. Time-temperature dependence of hardness changes in steel X 20 CrMoV 12 1.

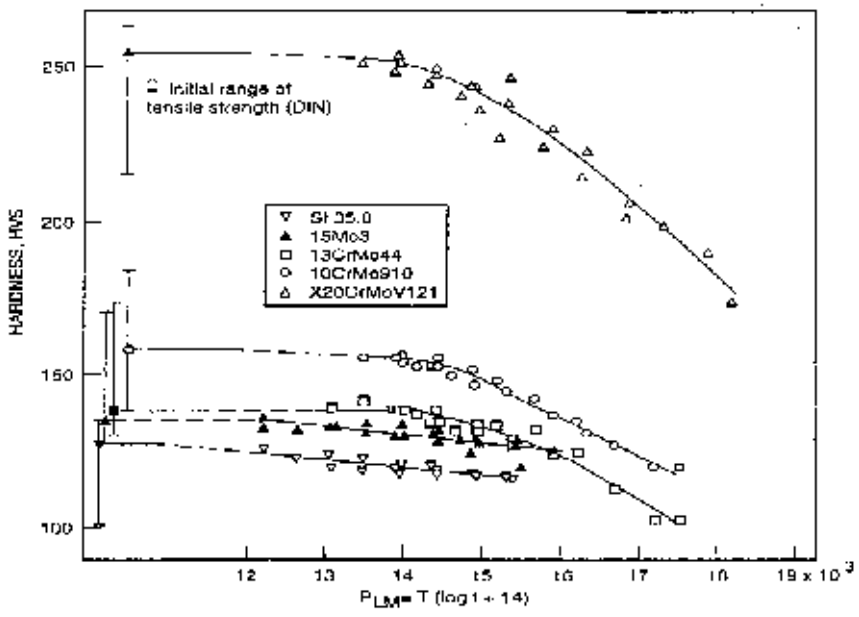

Fig. 12. Hardness as a function of the LM parameter of isothermal annealing.

The general trend of softening with increasing thermal exposure can be seen from Figure 12. Considerable scatter in the initial values of hardness are possible, although this is likely to be much less for small section boiler tubes than for thick section components. Therefore relative changes in hardness better reflect the thermal exposure than results from individual post-service hardness measurements.

A slight decrease in hardness was observed in steels St 35.8, 10 CrMo 9 10 and X 20 CrMoV 12 1 before any microstructural changes were observed using the methods of the present work. In steels 15 Mo 3 and 13 CrMo 4 4 the first signs of decreasing hardness and microstructural changes were coincidental.

In general, thermal exposure can be more accurately quantified from the microstructure than from the measured hardness. This is also true for cases where the original initial hardness and microstructure are not known, because of the relatively wider uncertainty in initial hardness than in the initial microstructures of boiler tubes.

3.3 IMPACT OF MICROSTRUCTURAL CHANGES

The boiler tube steels of the present work are mainly used for applications designed for creep resistance. The creep strength will decrease as thermal degradation proceeds, although the effect is much less pronounced at the relatively low service stress levels than in short-term laboratory testing. Also, the effects of degradation are inherently included in the long term creep testing results used for design. On the other hand, creep can also accelerate diffusionally driven microstructural degradation. The effect of stress (or strain) is modest by comparison with the influence of time and temperature, and at the usual low service stresses can be often neglected (Olson 1960; von Baerlecken & Fabritius 1966; Keller & Krisch 1977). Nevertheless, the general trend is decreasing creep strength with thermal degradation, which may take place slowly within normal service conditions or very quickly with overheating. Therefore, although even very extensive microstructural changes do not necessarily imply a threat to continued safe operation, unusually pronounced microstructural degradation suggests service conditions that shorten the expected service life markedly from the desired minimum life. The difference between expected and unusual levels of microstructural coarsening can be assessed and quantified by comparison with the example micrographs and the corresponding parametric estimates of the thermal service history.

4 SUMMARY

The thermal degradation of the microstructure of boiler steels St 35.8, 15 Mo 3, 13 CrMo 44, 10 CrMo 9 10 and X20 CrMoV 12 1 was investigated in the temperature range 600 - 780°C for up to 2 000 h. Direct metallography and hardness testing were used for characterising the microstructural changes and their time-temperature dependence. The results suggest a simple and consistent time-temperature dependence for all investigated materials, expected to apply also to long term service beyond the annealing time range of the present work. A collection of micrographs has been prepared to aid in classifying and evaluating the observed microstructural state in terms of isothermal service exposure at high temperature.

In general, the thermal exposure can be more accurately quantified from the microstructure than from the measured hardness. This is also true for cases where the original initial hardness and microstructure are not known, because of the relatively wider uncertainty in initial hardness than in the initial microstructures of boiler tubes.

REFERENCES

Borggreen, K. Experience from condition monitoring of steel type X 20 CrMoV 12 1 in life steam system. Baltica II - International Conference on Plant Life Management & Extension, Helsinki - Stockholm 5 - 6 October 1992. Espoo: Technical Research Centre of Finland, 1992. 13 p.

von Baerlecken, E. & Fabritius, H. Der Einfluß einer langzeitigen Glühung bei 500 bis 700°C auf das Kriechverhalten des Stahles 13 CrMo 44 bei 550°C. Arch. Eisenhüttenwesen, 1966. Vol. 37. Heft 7. Pp. 569 - 578.

Keller, H., & Krisch, A. Der Einfluss der Carbidausscheidungen auf das Kriechverhalten warmfester Chrom-Molybdän-Stähle. Arch. Eisenhüttenwesen, 1977. Vol. 48. Pp. 49 - 53.

Olson, K. G. Untersuchung der Kriechgeschwindigkeit eines Chrom-Molybdän Stahles in verschiedenen Wärmebehandlungszuständen. Bei int Aussprache über das Langzeitverhalten warmfester Stähle. Düsseldorf, 1960.

Toft, L. H. & Marsden, R. A. The structure and properties of 1% Cr-0.5% Mo steel after service in CEGB power stations. Structural processes in creep. London: ISI, 1961. P. 276 - 294. (ISI Spec. Rep. No. 70).

Viswanathan, R. Damage mechanisms and the life assessment of high-temperature components, USA 1989. Pp. 183 - 263.

OPTICAL MICROGRAPHS OF ISOTHERMALLY ANNEALED BOILER TUBE STEELS

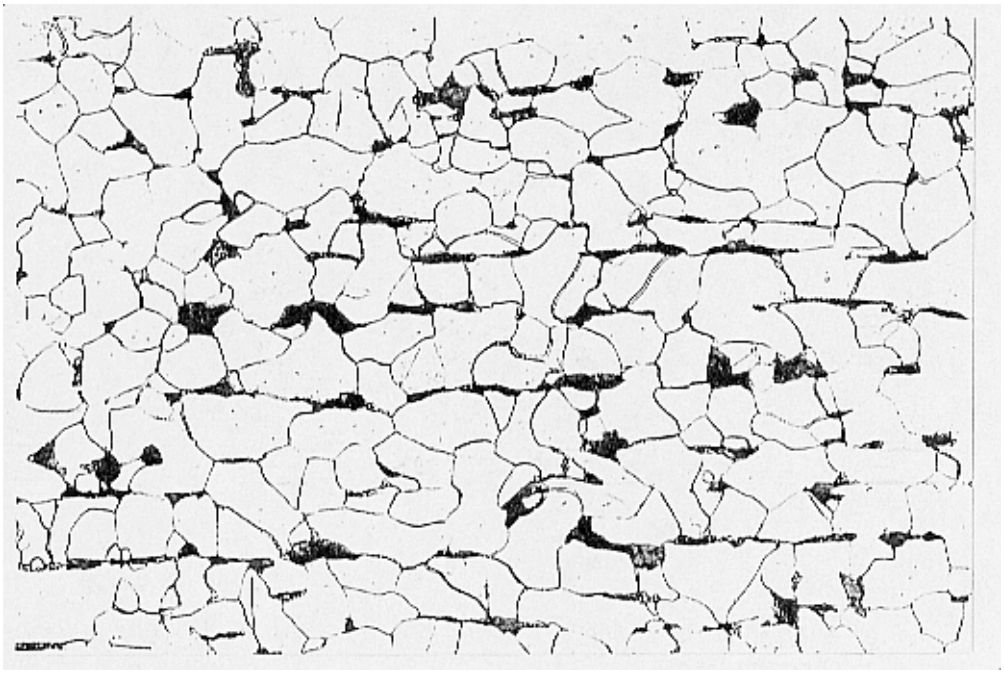

Fig. 1. Steel St 35.8: as new, stage A. Magnification 500x.

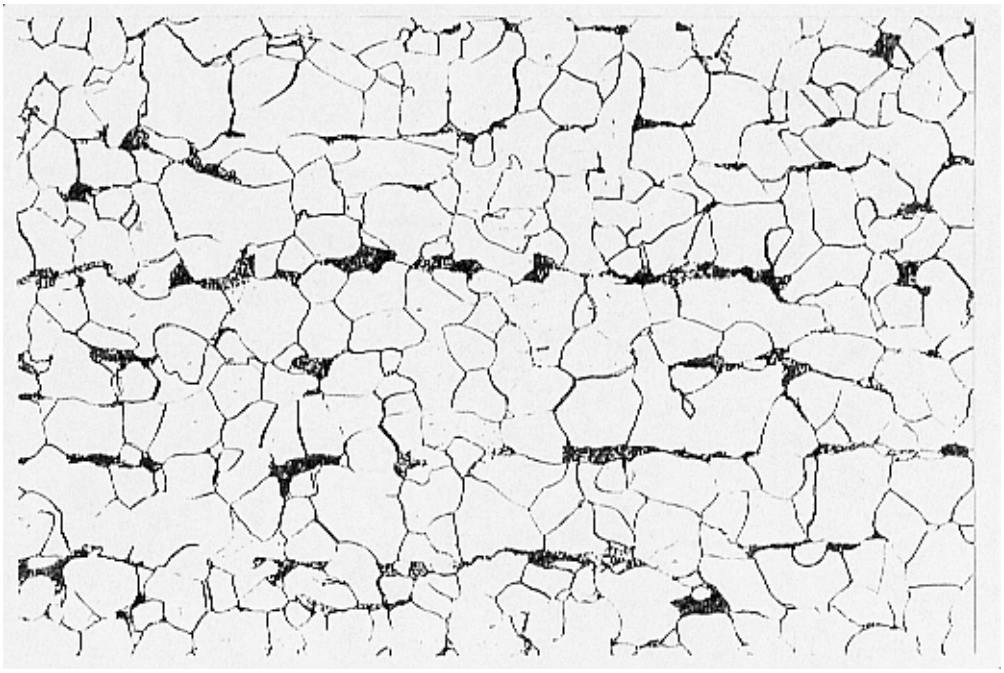

Fig. 2. Steel St 35.8: 600°C / 3 h, P_{LM} (C = 14) = 12 600, stage A/B. Magnification 500x.

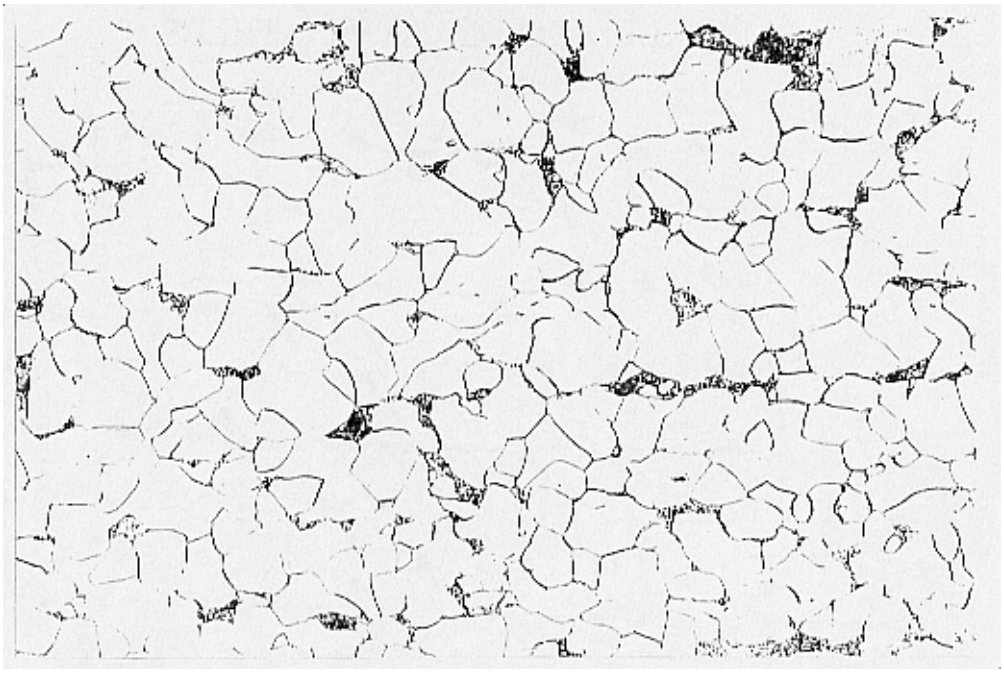

Fig. 3. Steel St 35.8: 600°C / 10 h, P_{LM} (C = 14) = 13 100, stage B. Magnification 500x.

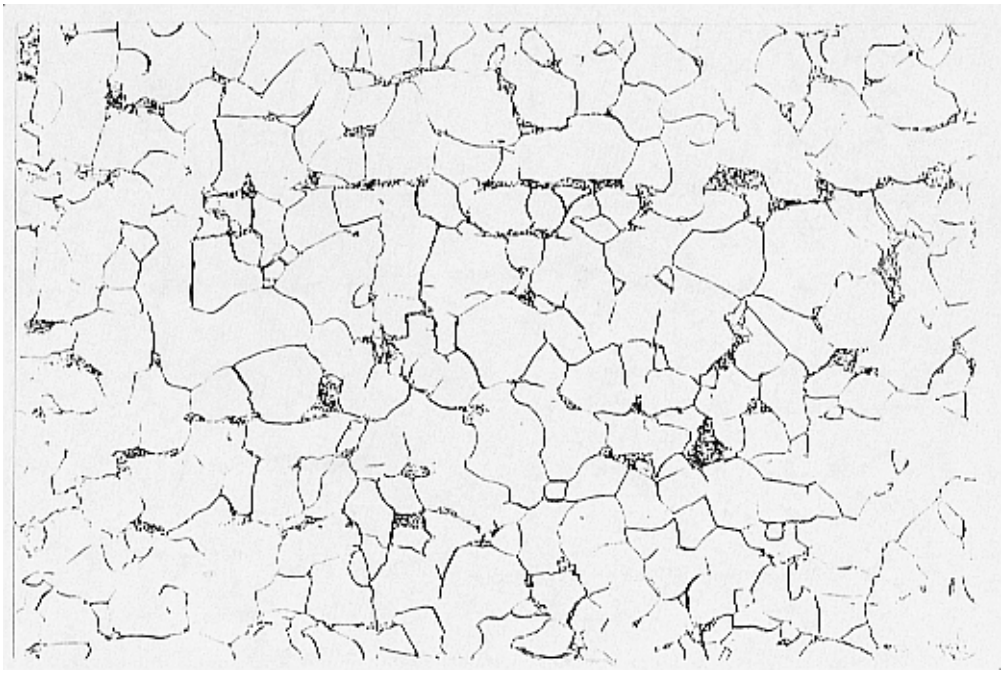

Fig. 4. Steel St 35.8: 600°C / 30 h, P_{LM} (C = 14) = 13 500, stage C. Magnification 500x.

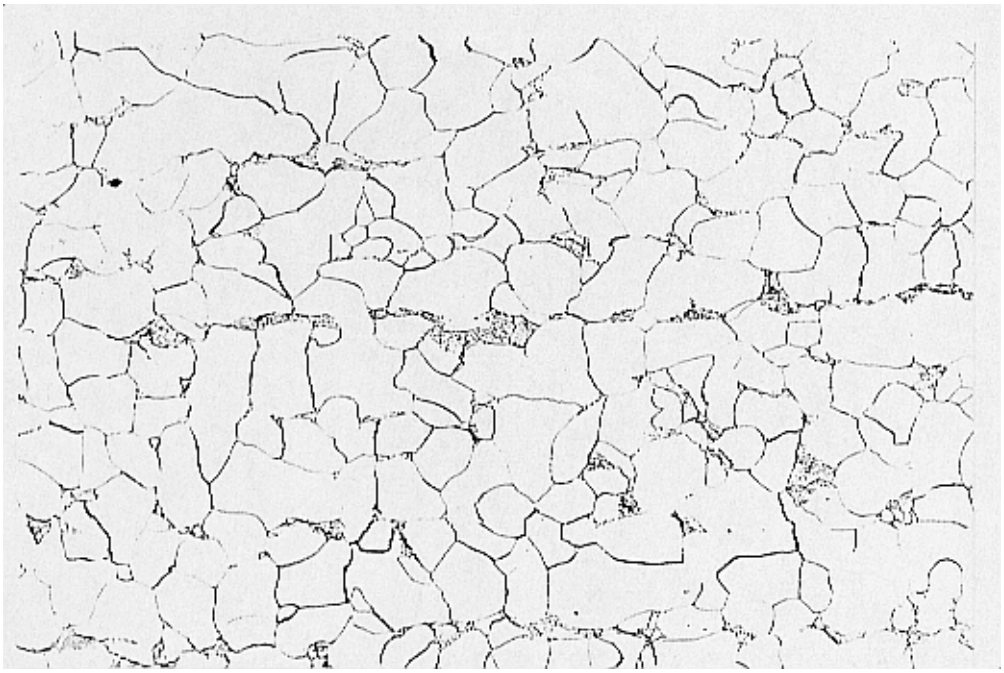

Fig. 5. Steel St 35.8: 600°C / 100 h, P_{LM} (C = 14) = 14 000, stage D. Magnification 500x.

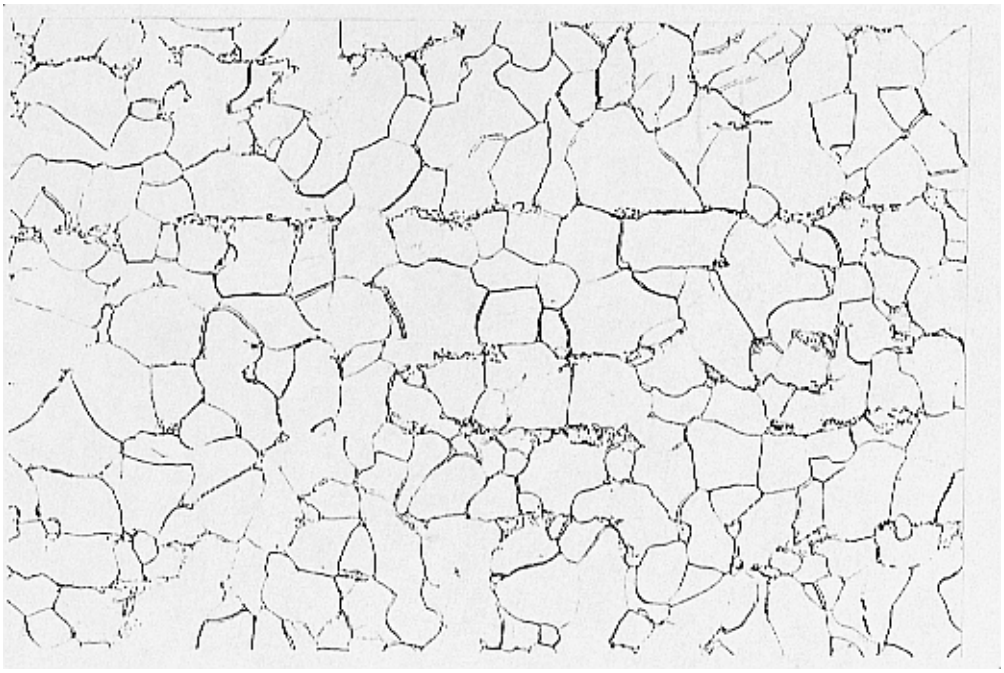

Fig. 6. Steel St 35.8: 600°C / 300 h, P_{LM} (C = 14) = 14 400, stage D. Magnification 500x.

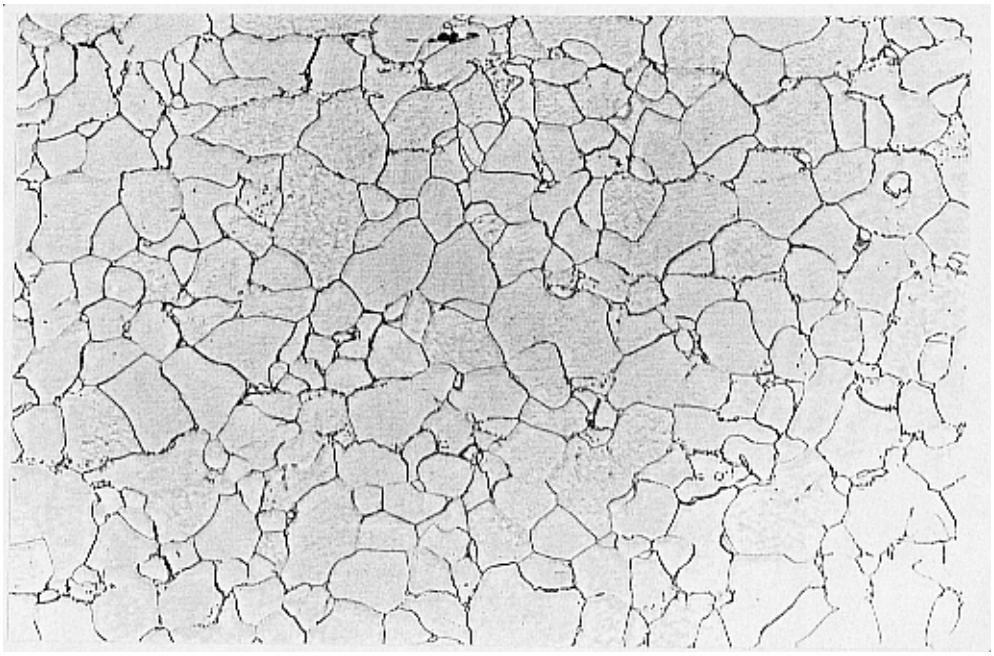

Fig. 7. Steel St 35.8: 720°C / 10 h, P_{LM} (C = 14) = 14 900, stage E. Magnification 500x.

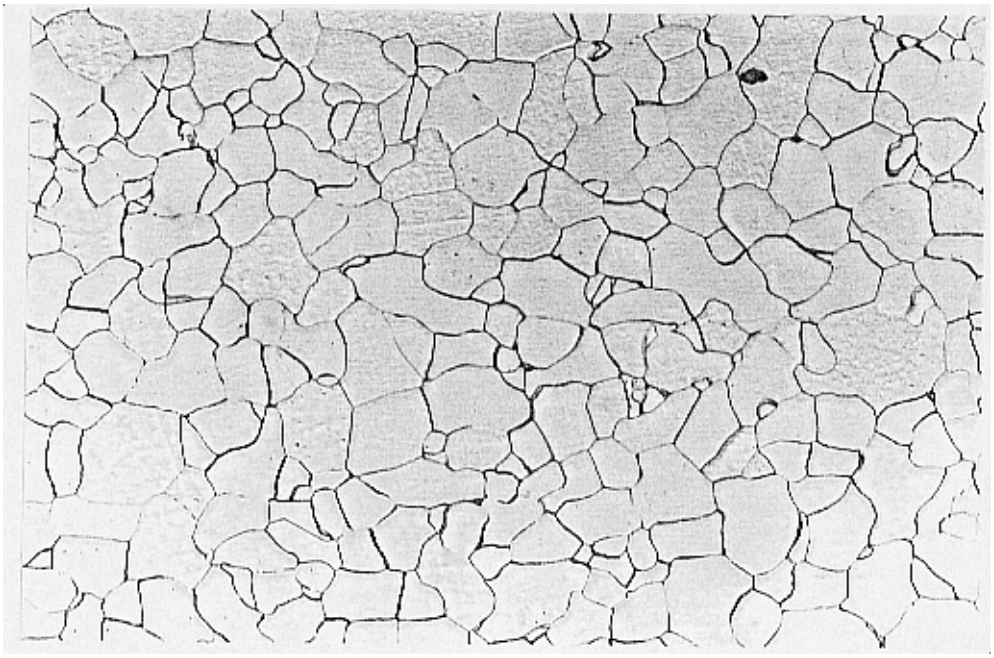

Fig. 8. Steel St 35.8: 720°C / 30 h, P_{LM} (C = 14) = 15 400, stage F. Magnification 500x.

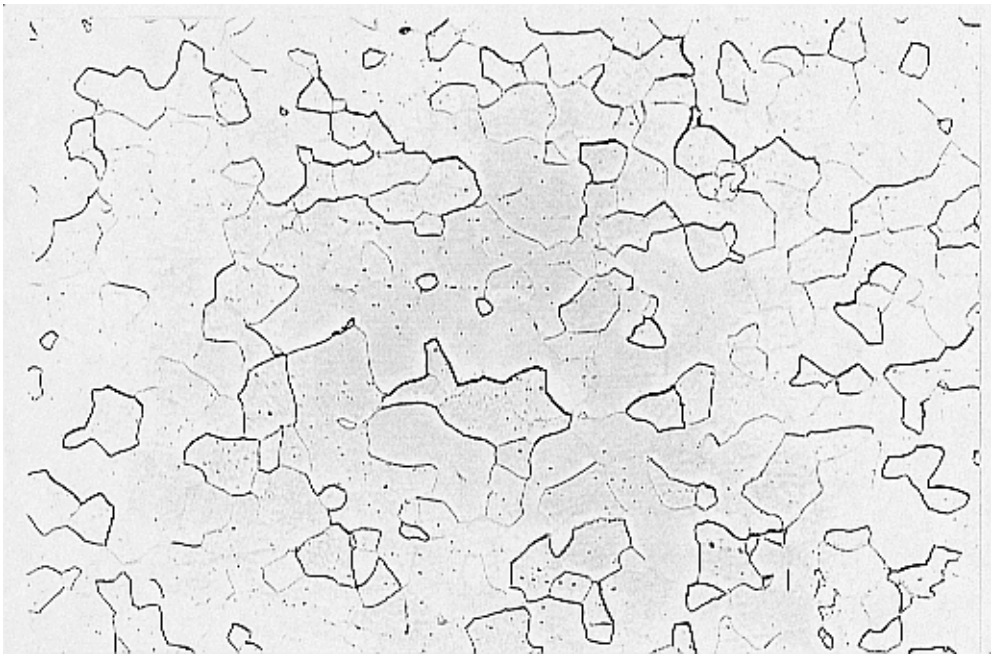

Fig. 9. Steel St 35.8: 720°C / 100 h, P_{LM} (C = 14) = 15 900, stage G. Magnification 500x.

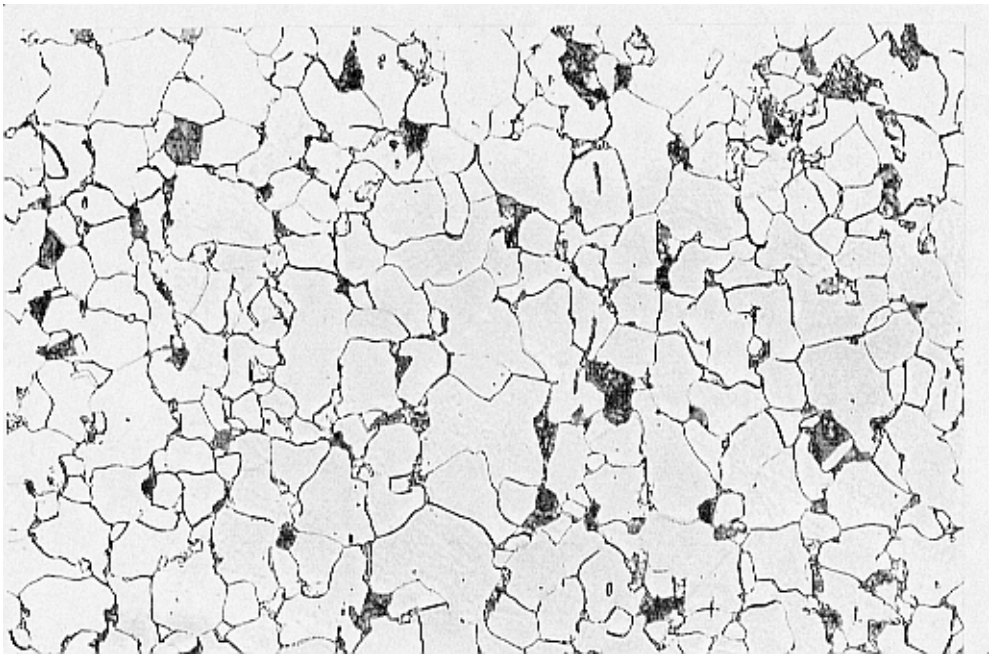

Fig. 10. Steel 15 Mo 3: as new, stage A. Magnification 500x.

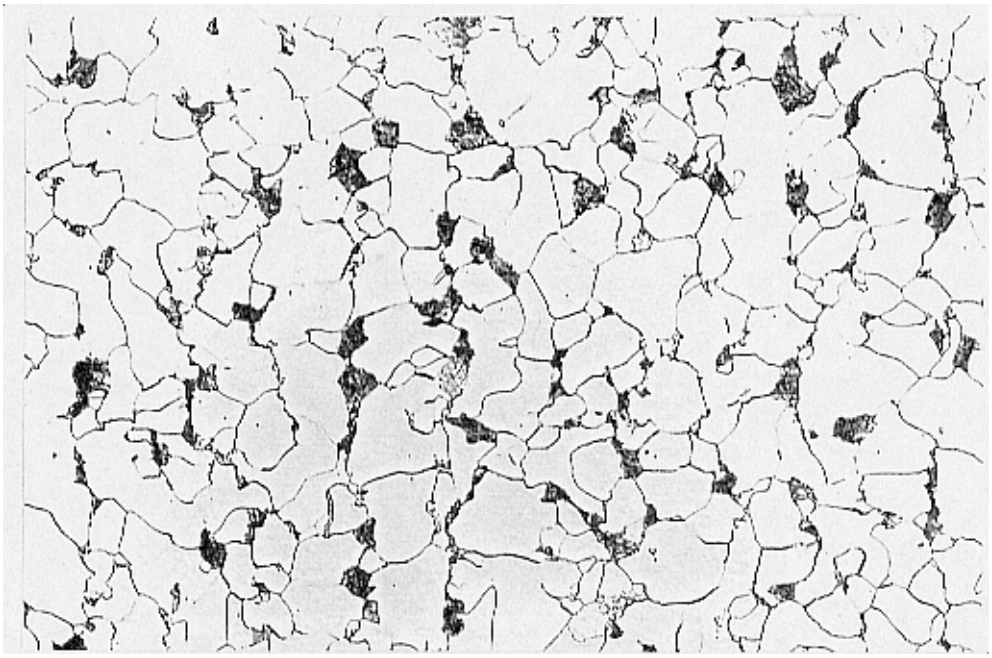

Fig. 11. Steel 15 Mo 3: 600°C / 30 h, P_{LM} (C = 14) = 13 500, stage B. Magnification 500x.

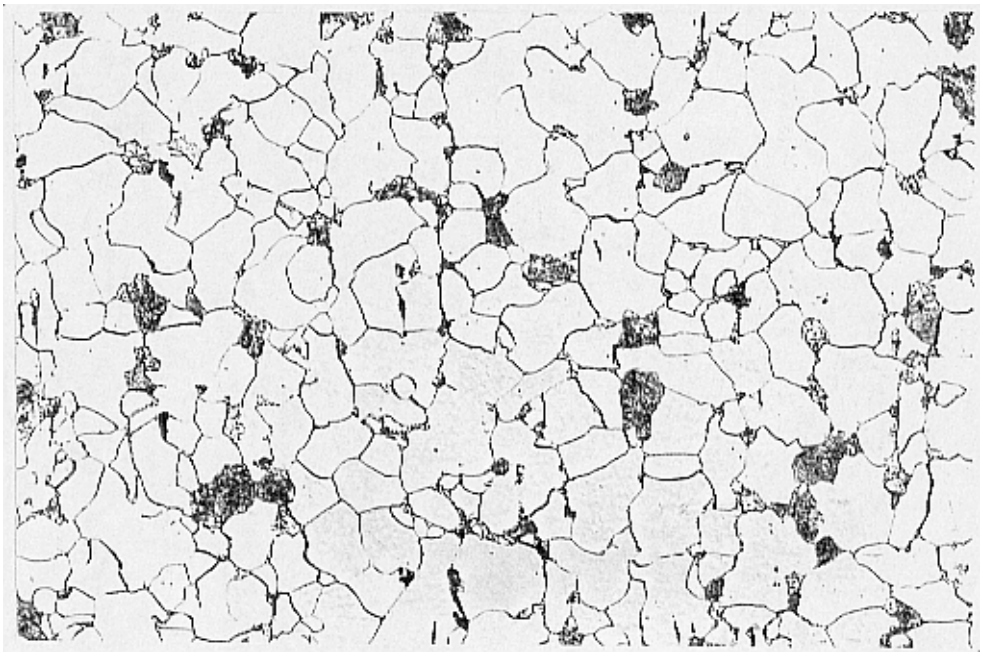

Fig. 12. Steel 15 Mo 3: 600°C / 100 h, P_{LM} (C = 14) = 14 000, stage C. Magnification 500x.

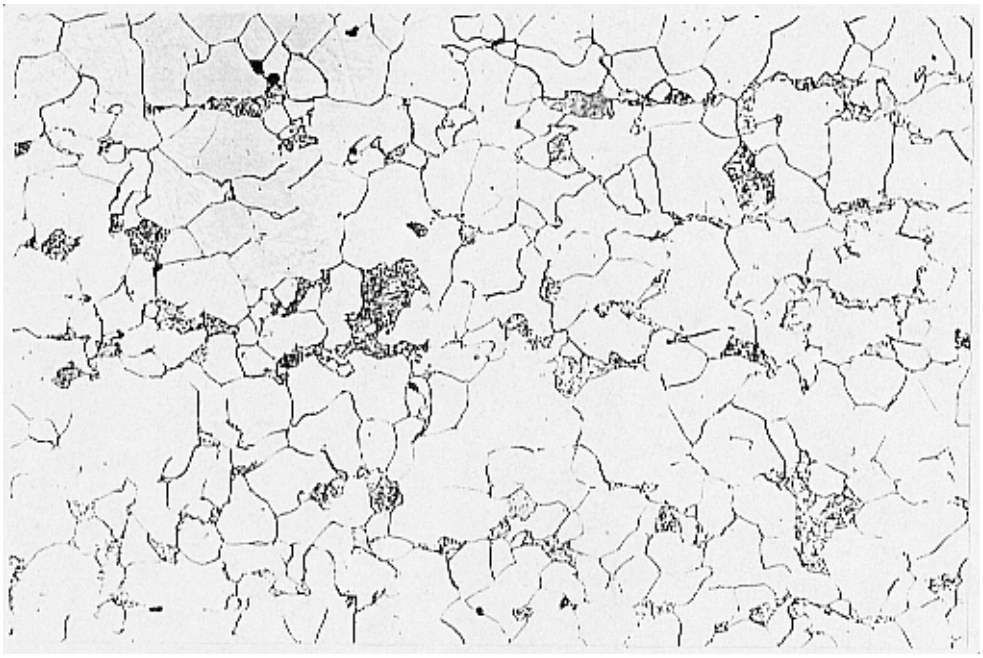

Fig. 13. Steel 15 Mo 3: 600°C / 300 h, P_{LM} (C = 14) = 14 400, stage D. Magnification 500x.

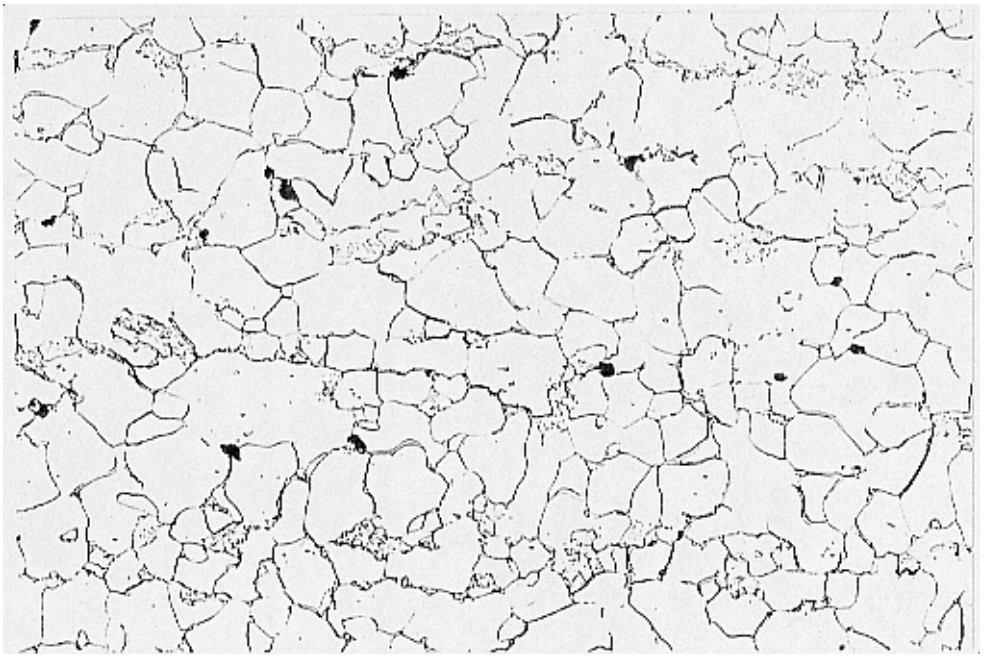

Fig. 14. Steel 15 Mo 3: 600°C / 1000 h, P_{LM} (C = 14) = 14 800, stage D. Magnification 500x. .

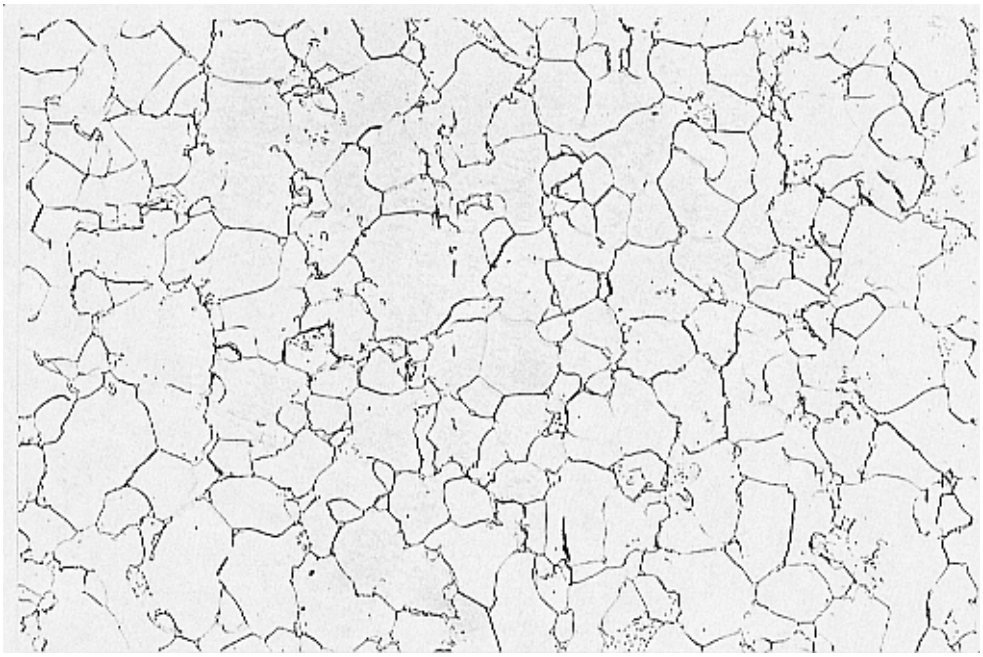

Fig. 15. Steel 15 Mo 3: 720°C / 30 h, P_{LM} (C = 14) = 15 400, stage E. Magnification 500x.

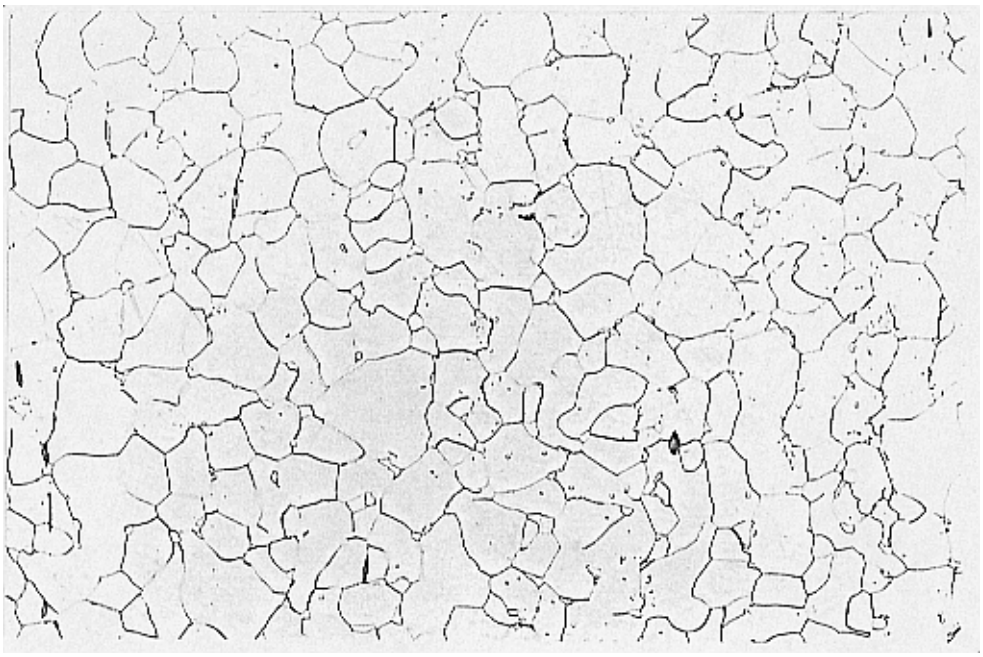

Fig. 16. Steel 15 Mo 3: 720°C / 100 h, P_{LM} (C = 14) = 15 900, stage F. Magnification 500x.

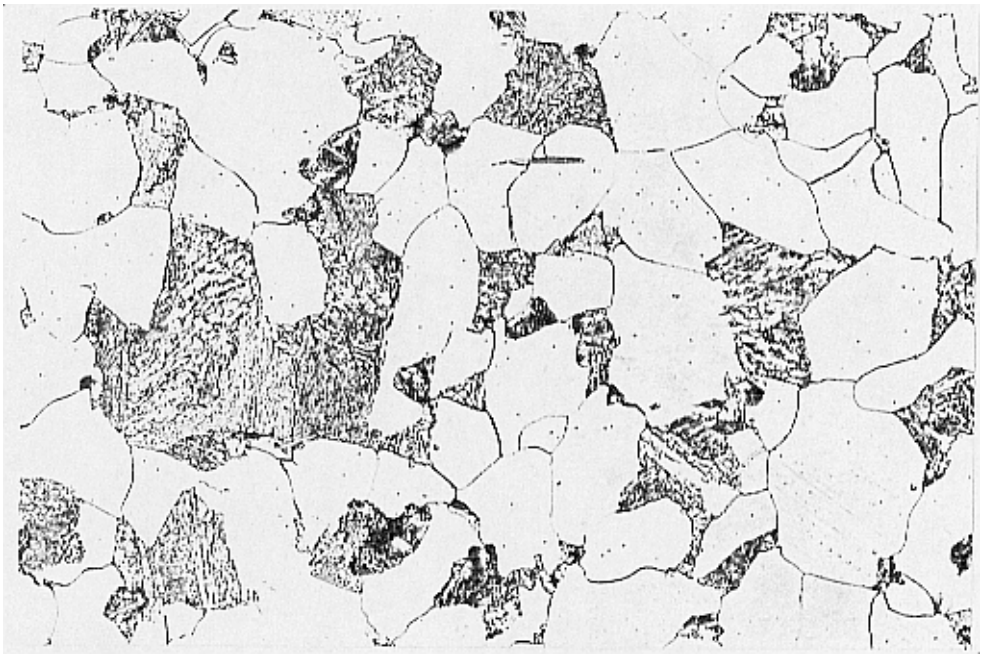

Fig. 17. Steel 13 CrMo 4 4: as new, stage B. Magnification 500x.

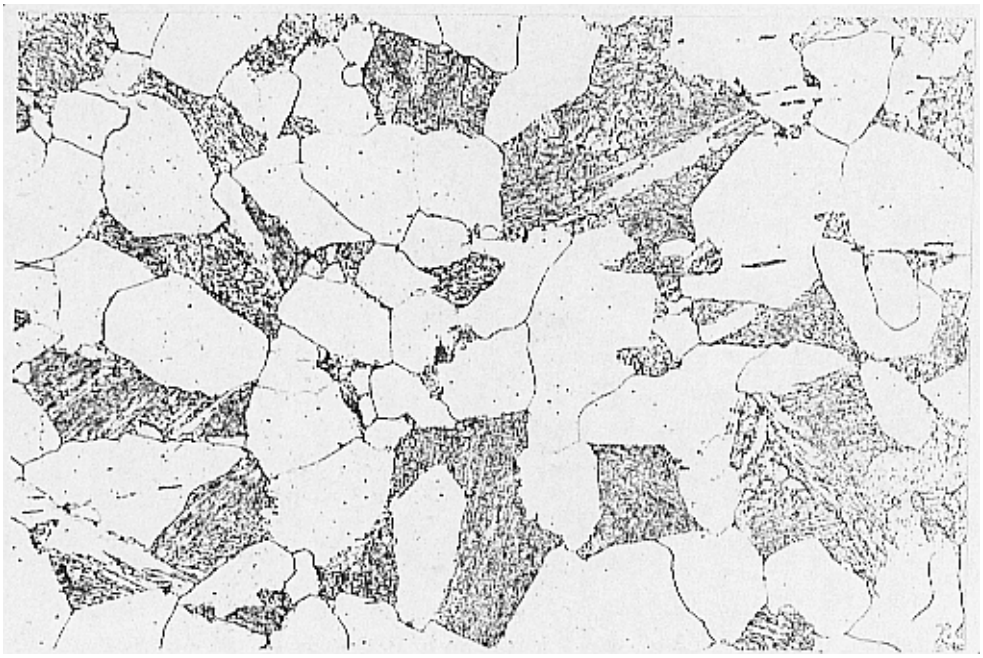

Fig. 18. Steel 13 CrMo 4 4: 720°C / 3 h, P_{LM} (C = 12) = 12 400, P_{LM} (C = 14) = 14 400, stage B. Magnification 500x.

Fig. 19. Steel 13 CrMo 4 4: 720°C / 10 h, P_{LM} (C = 12) = 12 900, P_{LM} (C = 14) = 14 900, stage C. Magnification 500x.

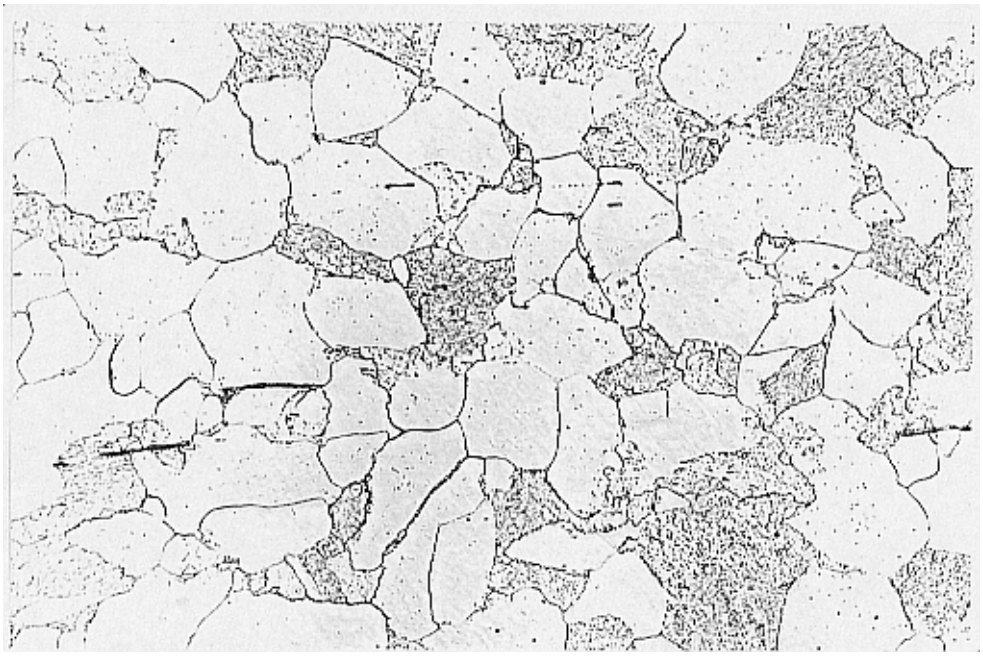

Fig. 20. Steel 13 CrMo 4 4: 720°C / 30 h, P_{LM} (C = 12) = 13 400, P_{LM} (C = 14) = 15 400, stage D. Magnification 500x.

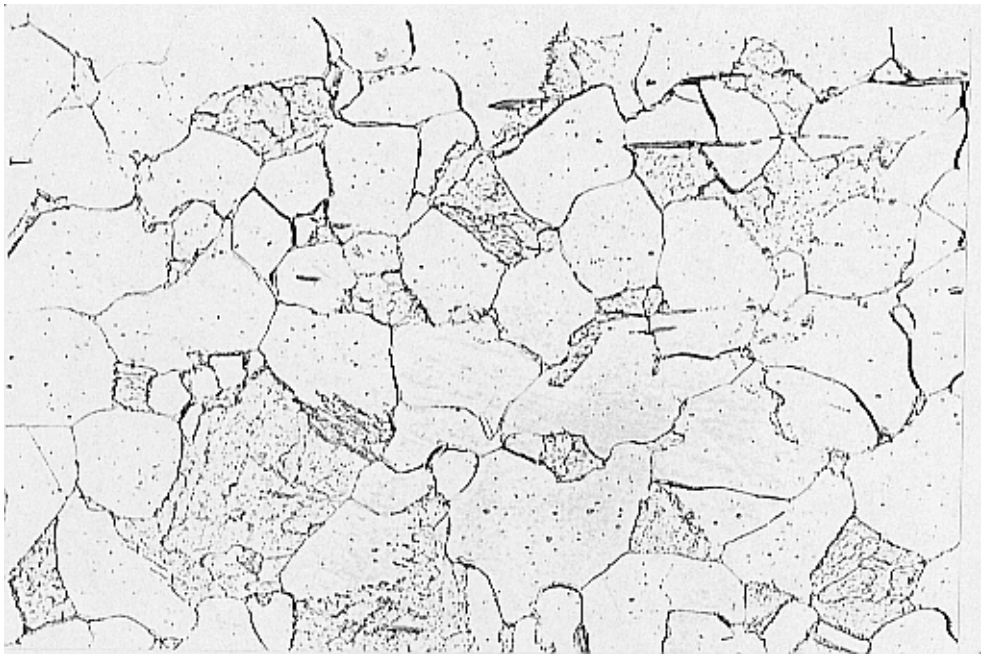

Fig. 21. Steel 13 CrMo 4 4: 720°C / 100 h, P_{LM} (C = 12) = 13 900, P_{LM} (C = 14) = 15 900, stage E. Magnification 500x.

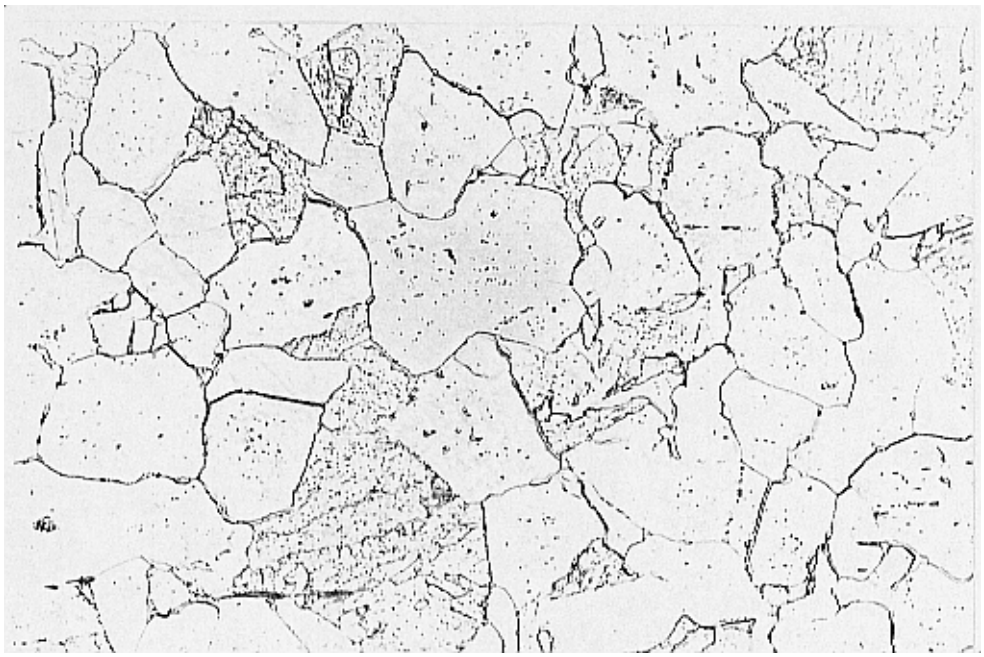

Fig. 22. Steel 13 CrMo 4 4: 740°C / 100 h, P_{LM} (C = 12) = 14 200, P_{LM} (C = 14) = 16 200, stage E. Magnification 500x.

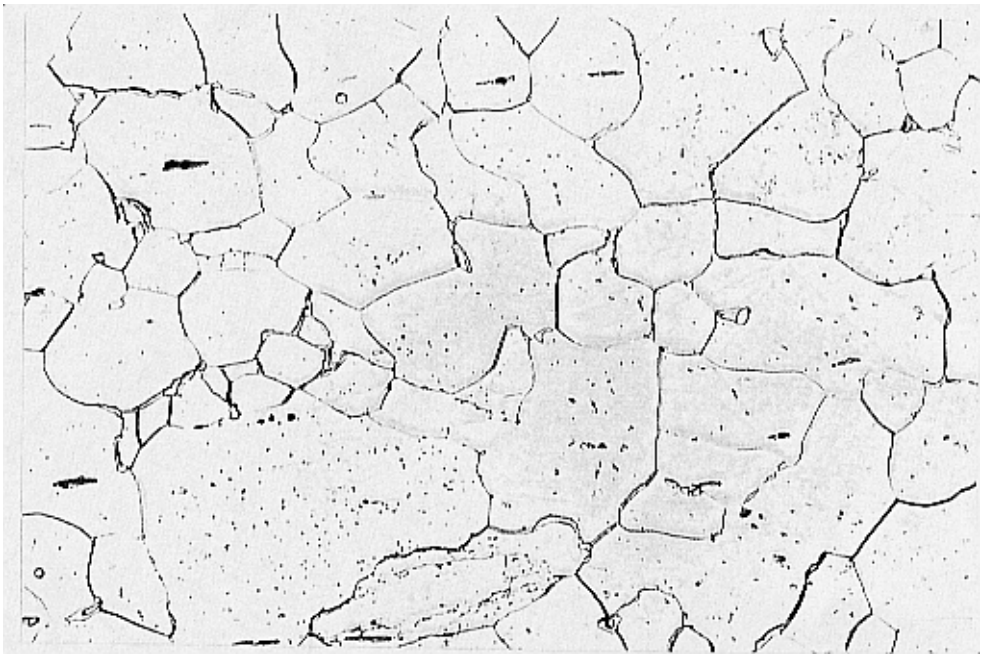

Fig. 23. Steel 13 CrMo 4 4: 740°C / 300 h, P_{LM} (C = 12) = 14 700, P_{LM} (C = 14) = 16 700, stages E/F. Magnification 500x.

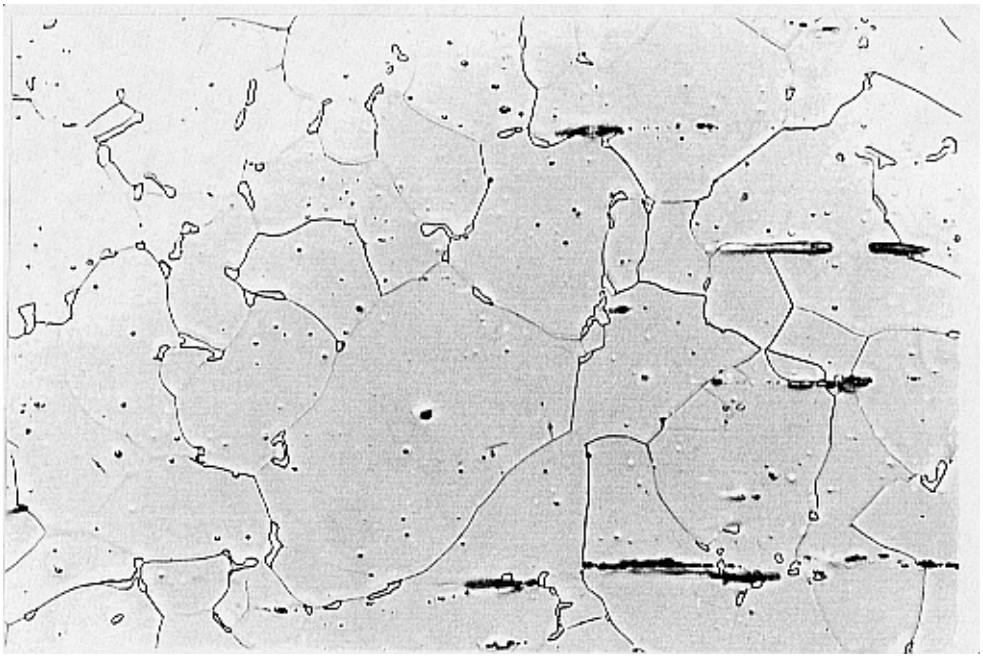

Fig. 24. Steel 13 CrMo 4 4: 740°C / 1000 h, P_{LM} (C = 12) = 15 200, P_{LM} (C = 14) = 17 200, stage F. Magnification 500x.

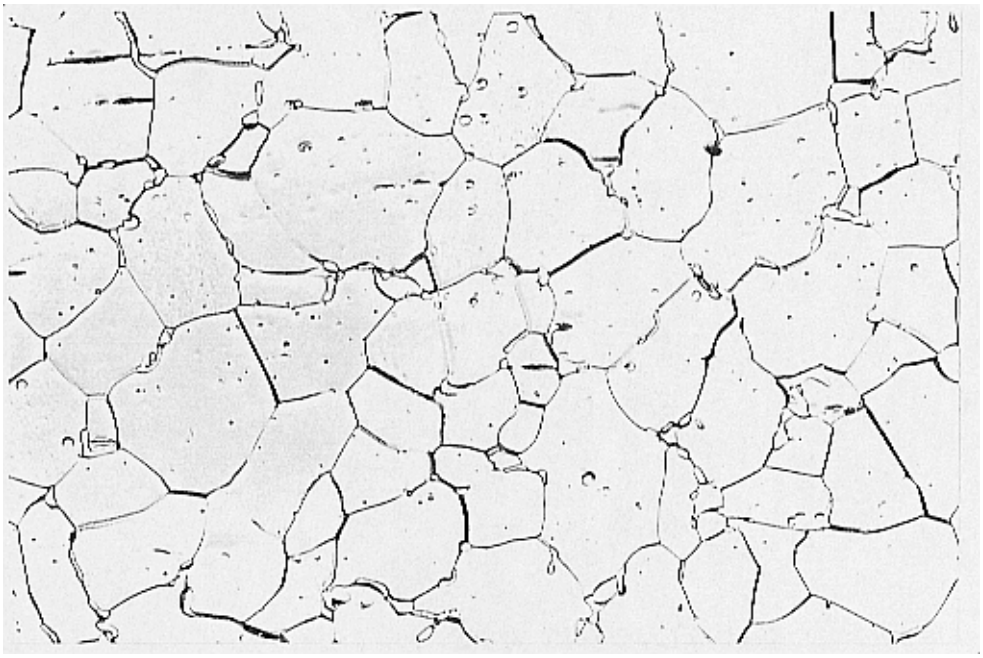

Fig. 25. Steel 13 CrMo 4 4: 740°C / 2000 h, P_{LM} (C = 12) = 15 500, P_{LM} (C = 14) = 17 500, stage F. Magnification 500x.

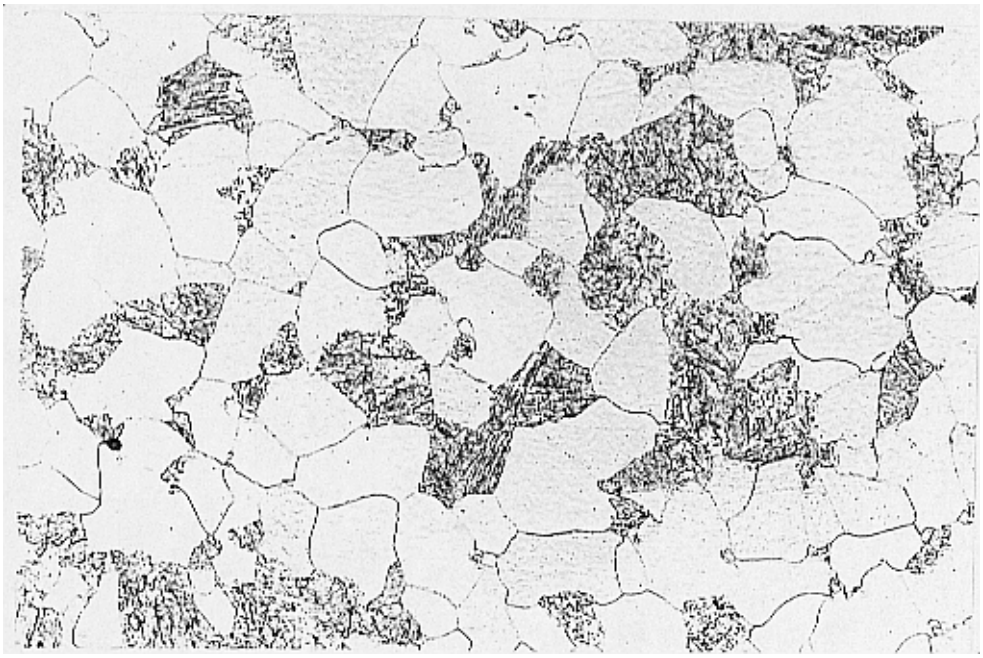

Fig. 26. Steel 10 CrMo 9 10: as new, stage B. Magnification 500x.

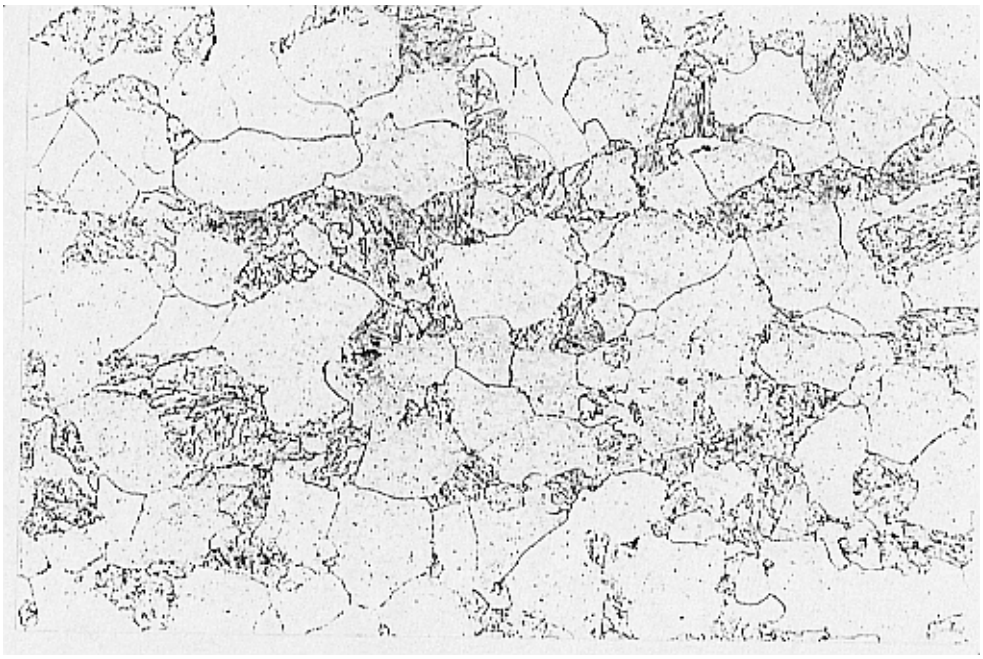

Fig. 27. Steel 10 CrMo 9 10: 720°C / 3 h, P_{LM} (C = 14) = 14 400, stage B/C. Magnification 500x.

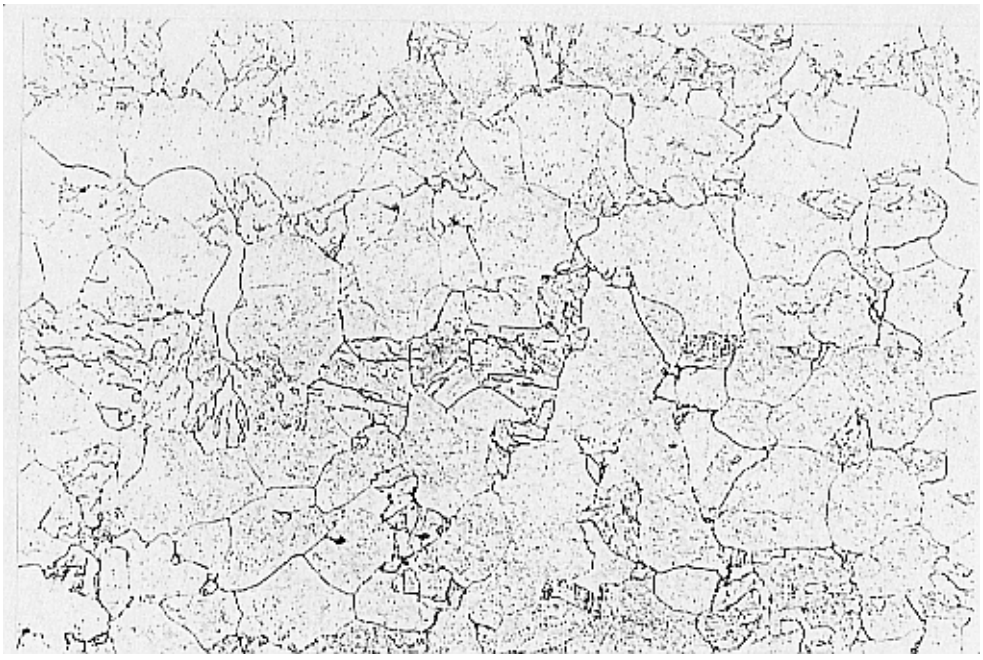

Fig. 28. Steel 10 CrMo 9 10: 720°C / 10 h, P_{LM} (C = 14) = 14 900, stage C. Magnification 500x.

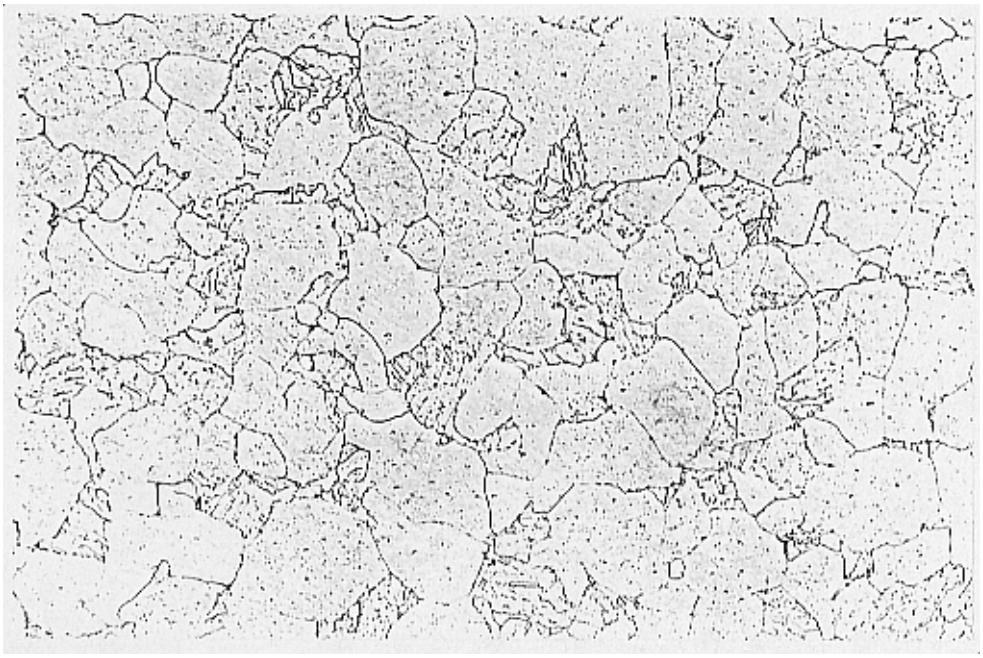

Fig. 29. Steel 10 CrMo 9 10: 720°C / 30 h, P_{LM} (C = 14) = 15 400, stage D. Magnification 500x.

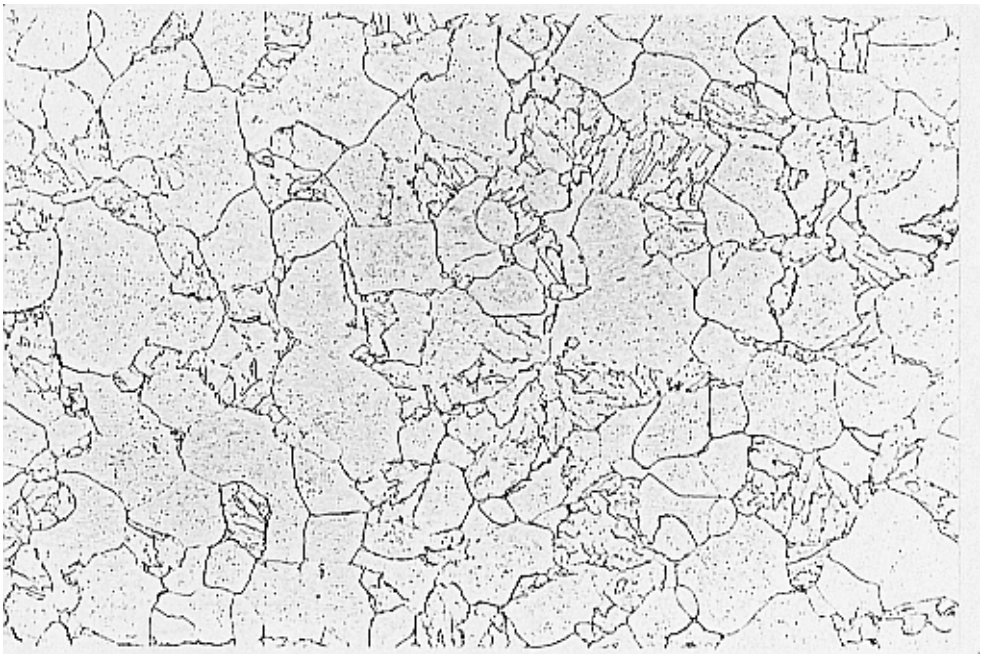

Fig. 30. Steel 10 CrMo 9 10: 720°C / 100 h, P_{LM} (C = 14) = 15 900, stage D. Magnification 500x.

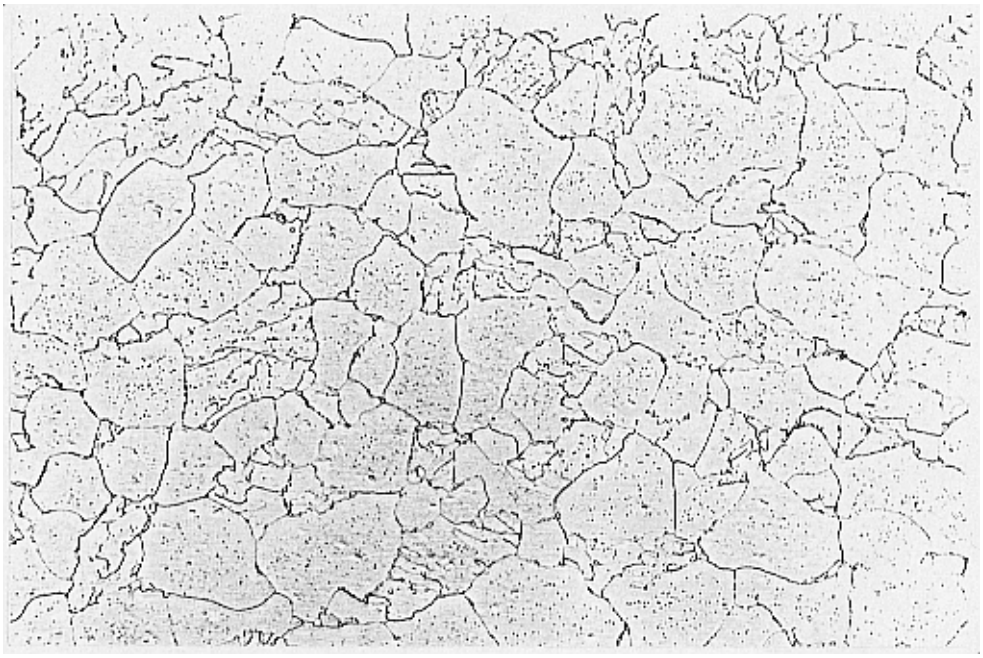

Fig. 31. Steel 10 CrMo 9 10: 720°C / 300 h, P_{LM} (C = 14) = 16 400, stage E. Magnification 500x.

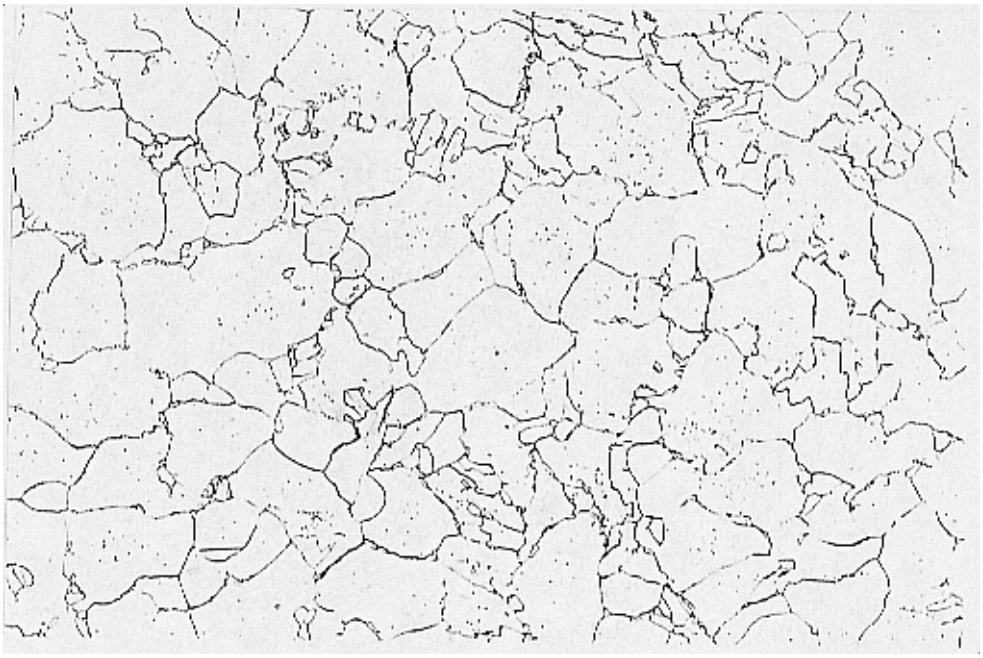

Fig. 32. Steel 10 CrMo 9 10: 740°C / 300 h, P_{LM} (C = 14) = 16 700, stage E. Magnification 500 x.

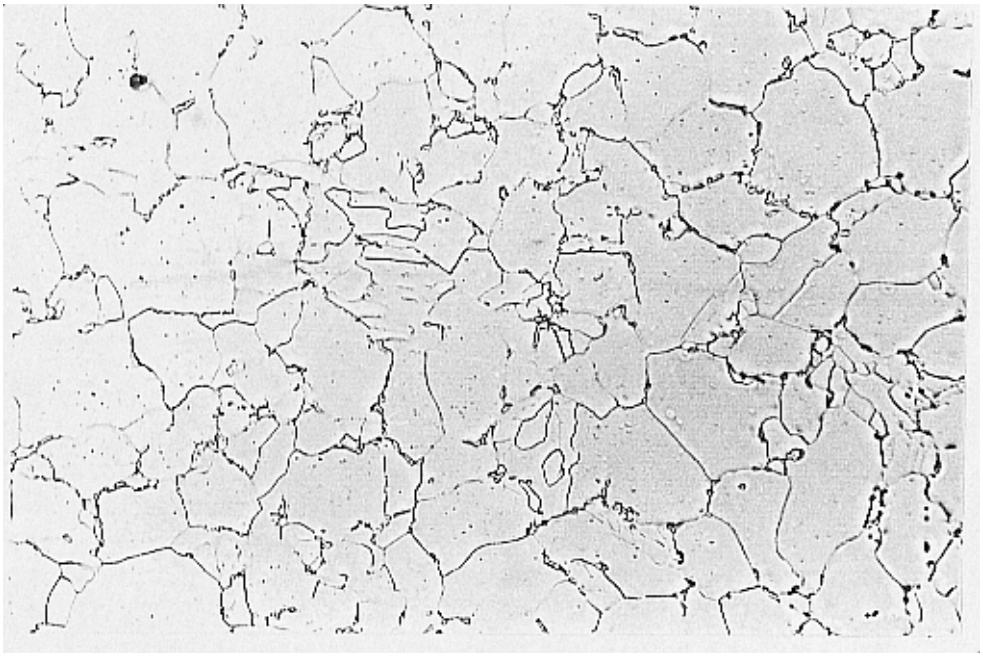

Fig. 33. Steel 10 CrMo 9 10: 740°C / 1000 h, P_{LM} (C = 14) = 17 200, stage E/F. Magnification 500 x.

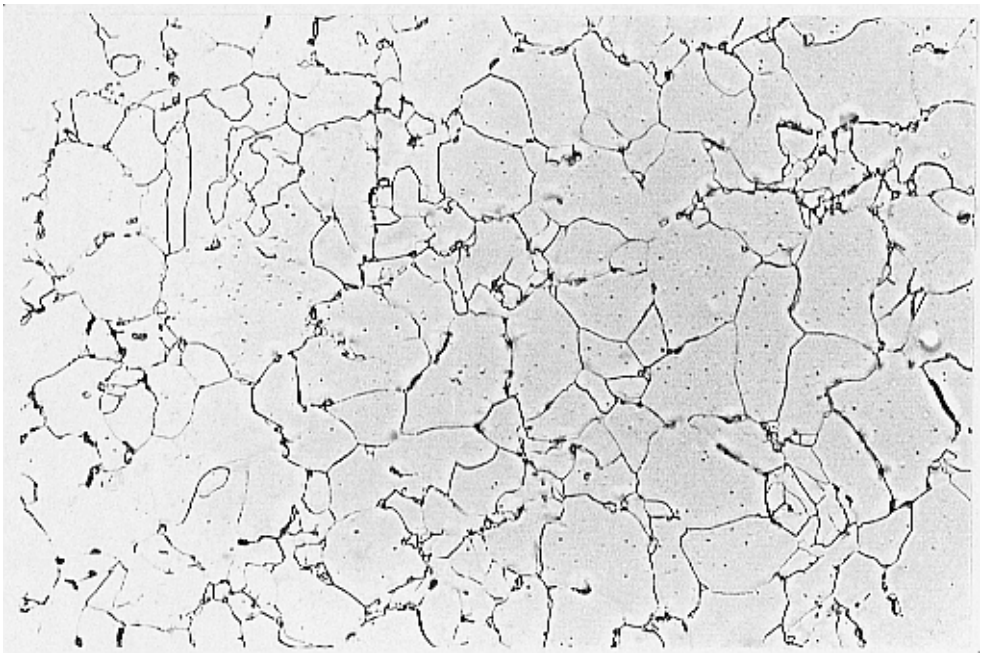

Fig. 34. Steel 10 CrMo 9 10: 740°C / 2000 h, P_{LM} (C = 14) = 17 500, stage F. Magnification 500x.

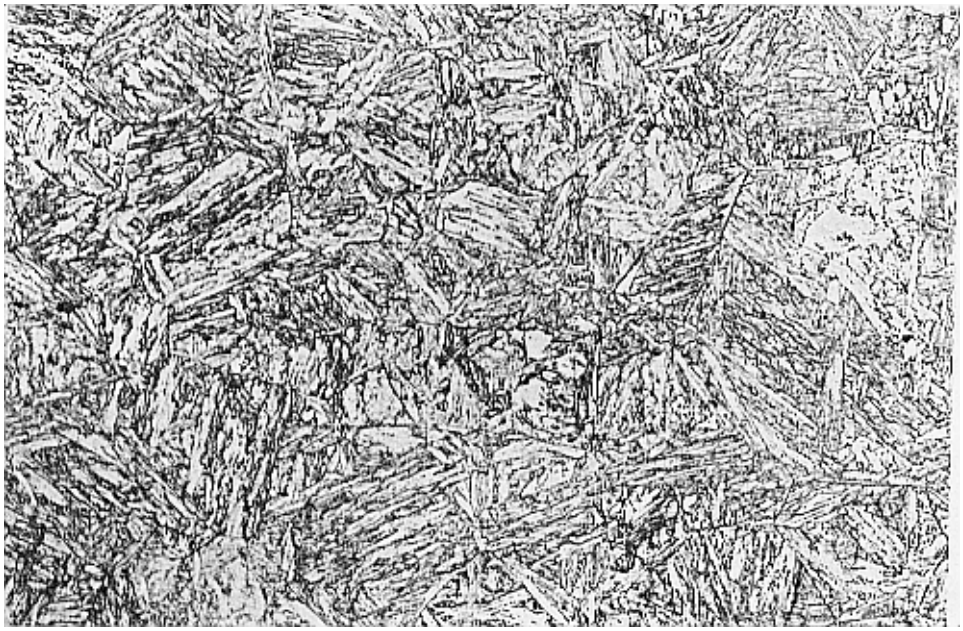

Fig. 35. Steel X 20 CrMoV 12 1: as new, stage B. Magnification 500x.

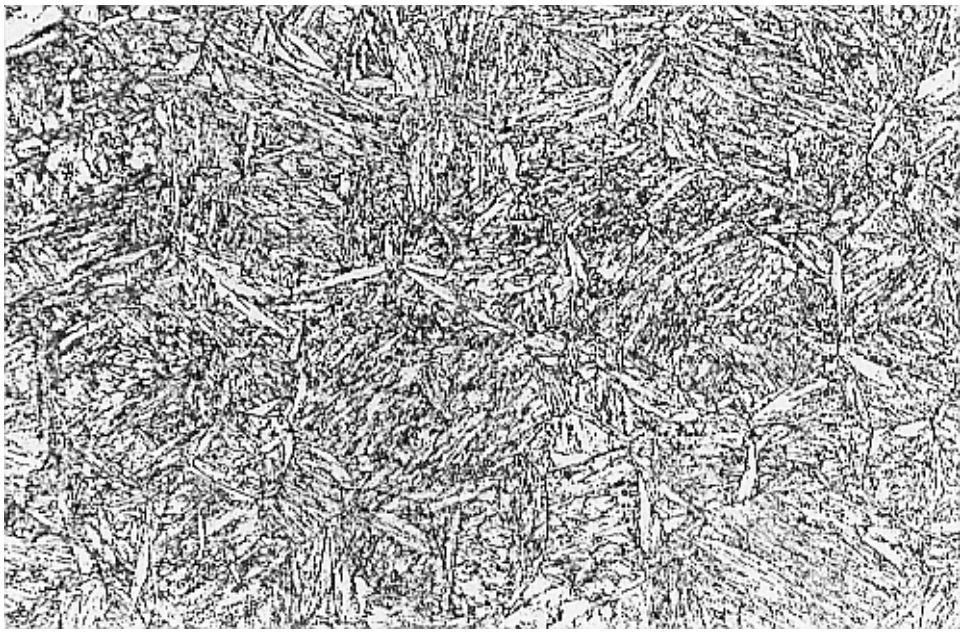

Fig. 36. Steel X 20 CrMoV 12 1: 720°C / 10 h, P_{LM} (C = 14) = 14 900, stage B. Magnification 500x.

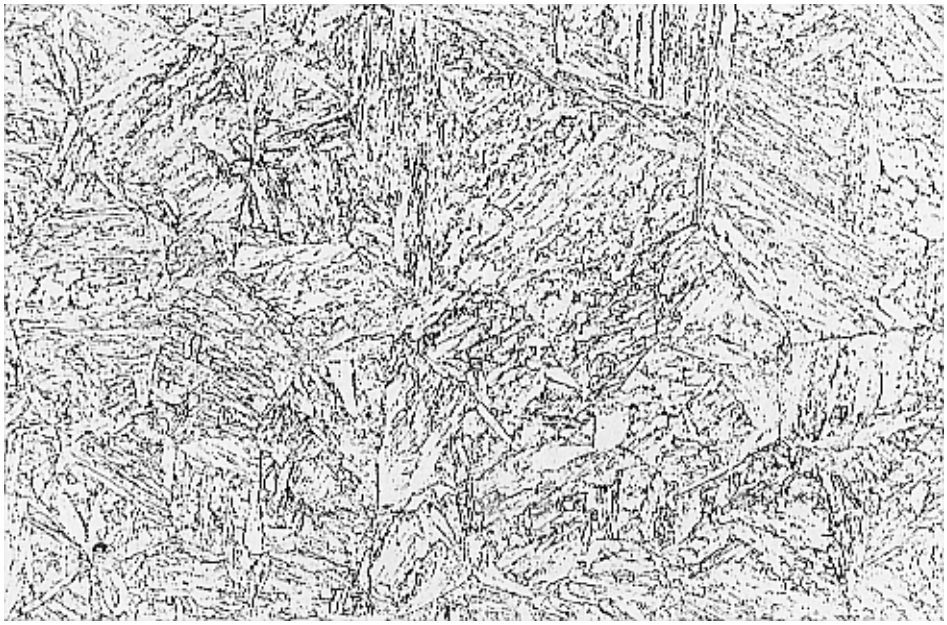

Fig. 37. Steel X 20 CrMoV 12 1: 780°C / 3 h, P_{LM} (C = 14) = 15 200, stage B/C. Magnification 500x.

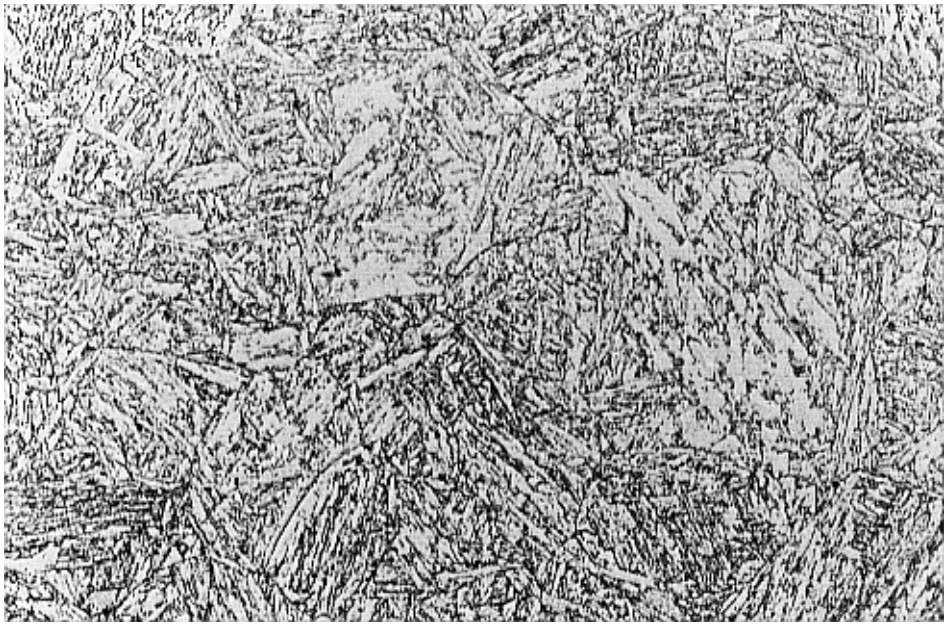

Fig. 38. Steel X 20 CrMoV 12 1: 780°C / 10 h, P_{LM} (C = 14) = 15 800, stage C. Magnification 500x.

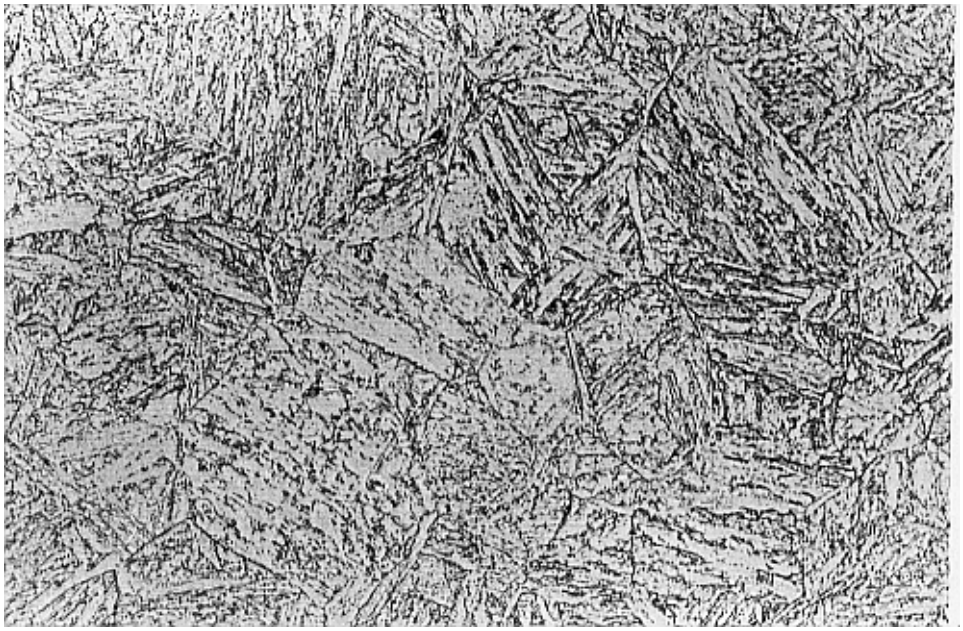

Fig. 39. Steel X 20 CrMoV 12 1: 780°C / 30 h, P_{LM} (C = 14) = 16 300, stage D. Magnification 500x.

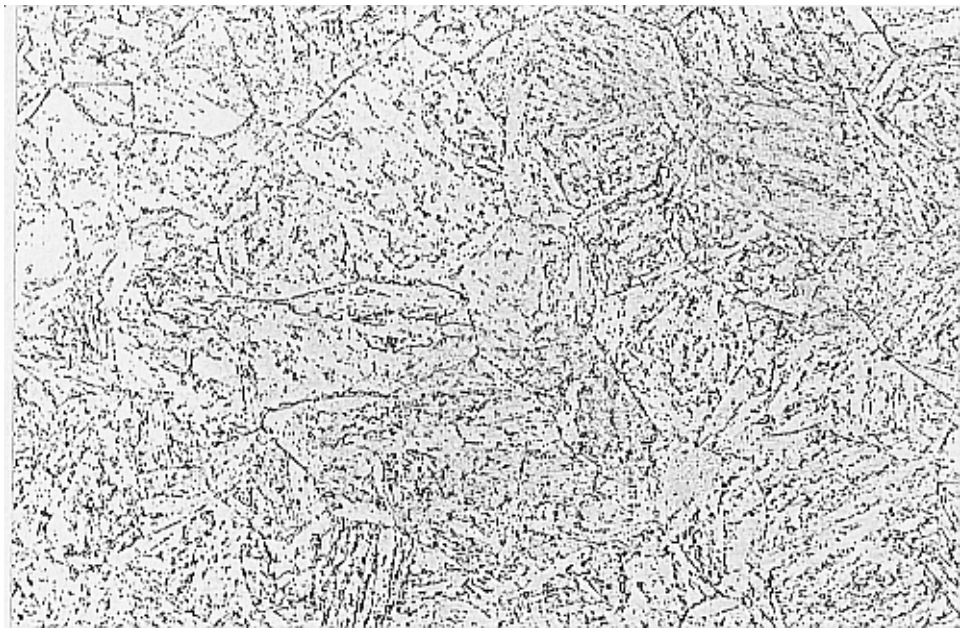

Fig. 40. Steel X 20 CrMoV 12 1: 780°C / 100 h, P_{LM} (C = 14) = 16 800, stage E. Magnification 500x.

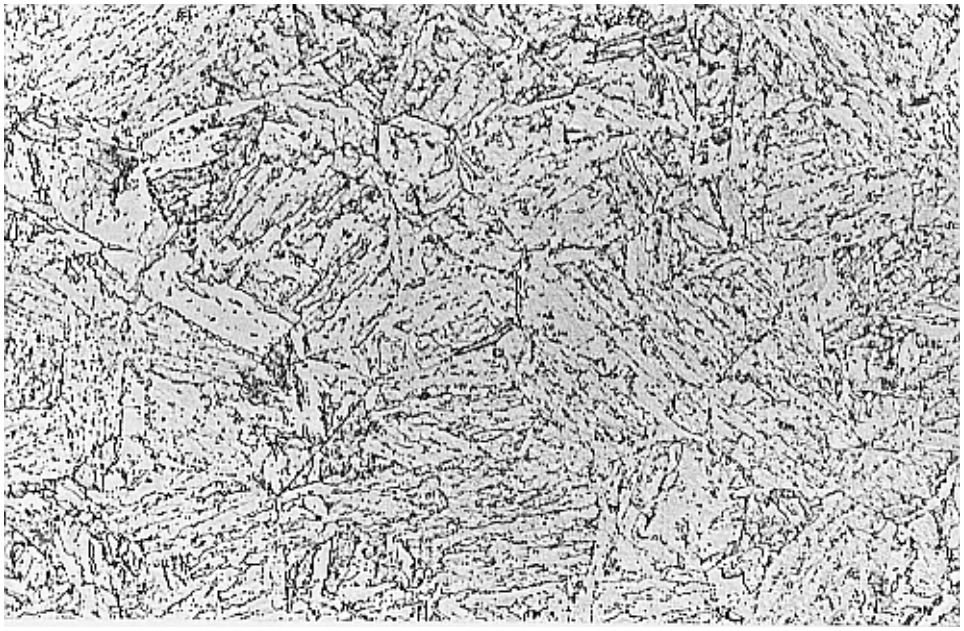

Fig. 41. Steel X 20 CrMoV 12 1: 780°C / 300 h, P_{LM} (C = 14) = 17 400, stage E. Magnification 500x.

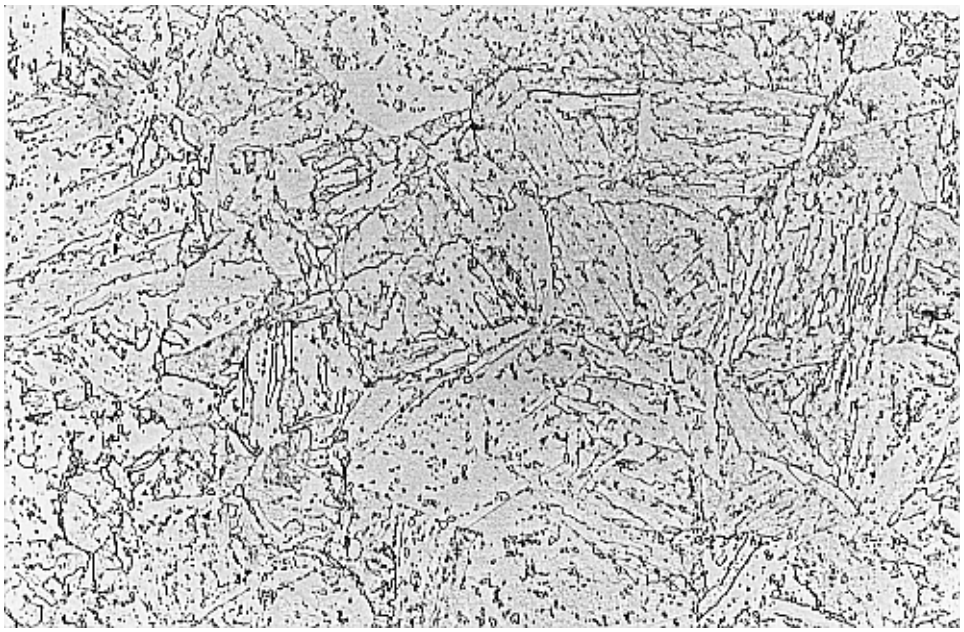

Fig. 42. Steel X 20 CrMoV 12 1, 780°C, 1000 h, P_{LM} (C = 14) = 17 900, stage E. Magnification 500x.

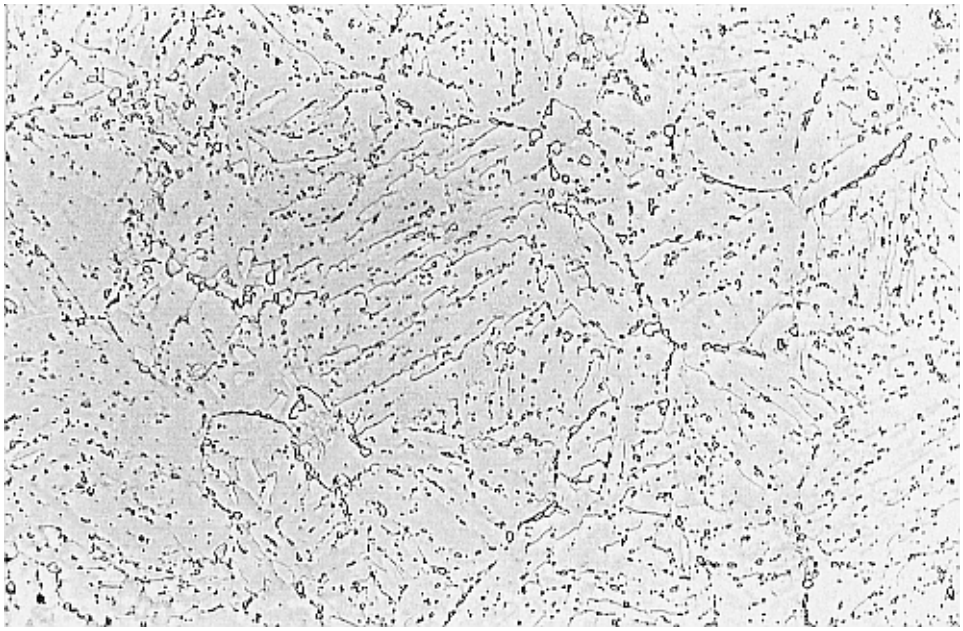

Fig. 43. Steel X 20 CrMoV 12 1: 780°C / 2000 h, P_{LM} (C = 14) = 18 200, stage E. Magnification 500x.

SCANNING ELECTRON MICROGRAPHS OF ANNEALED BOILER TUBE STEELS

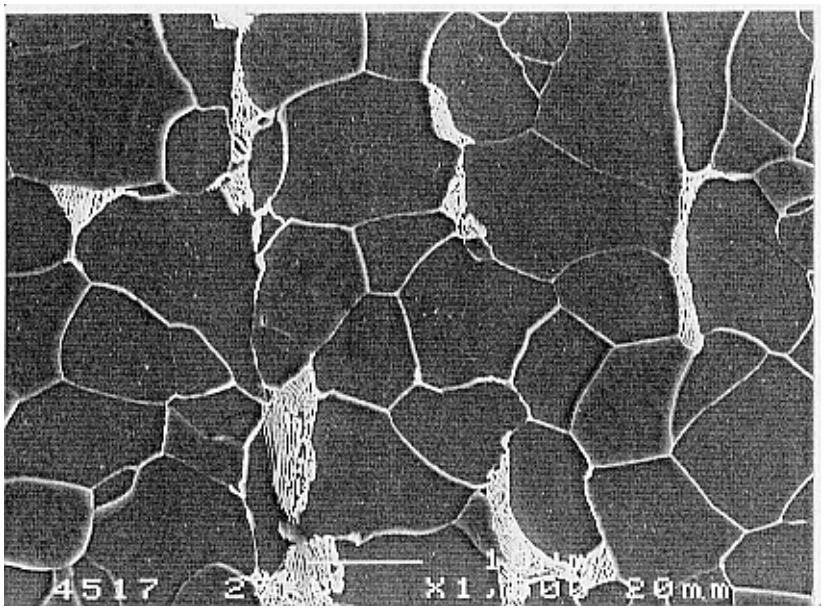

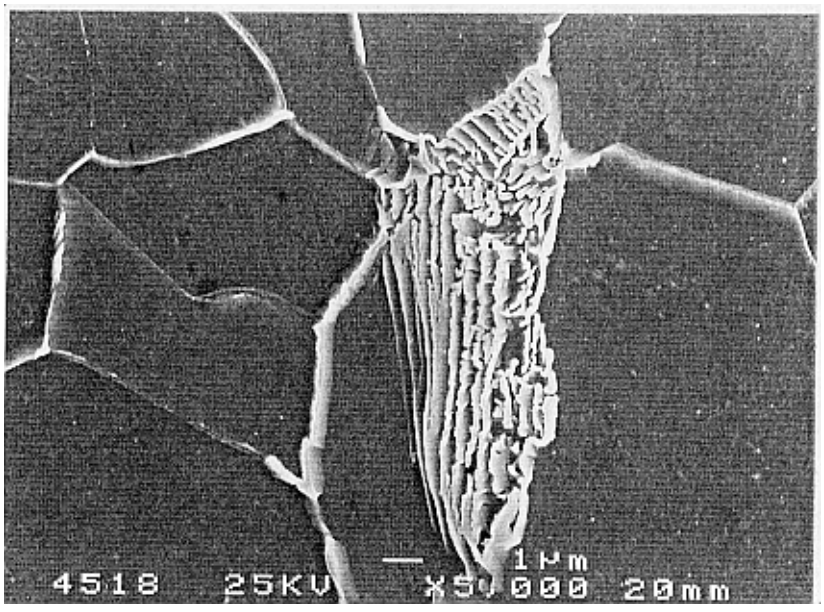

Figs. 1 and 2. Steel St 35.8: as new, stage A. Magnification 1500x (Fig. 1) and 5000x (Fig. 2).

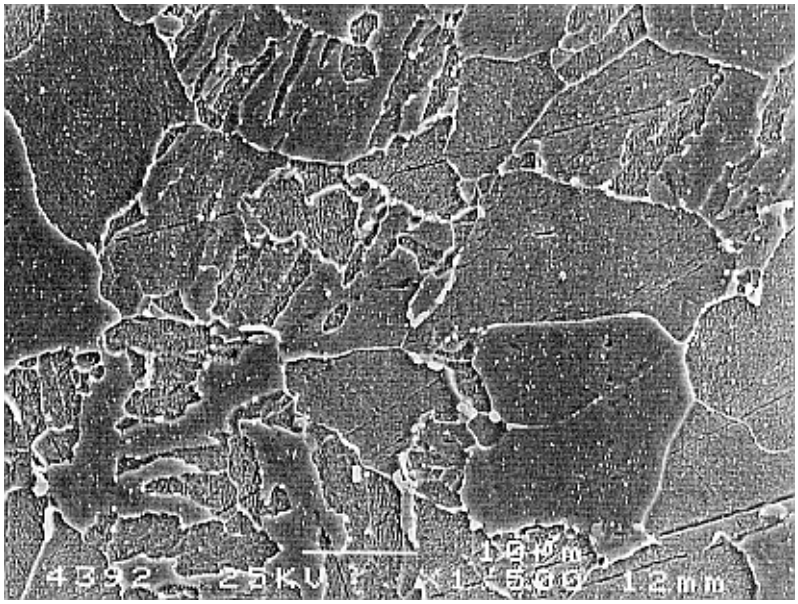

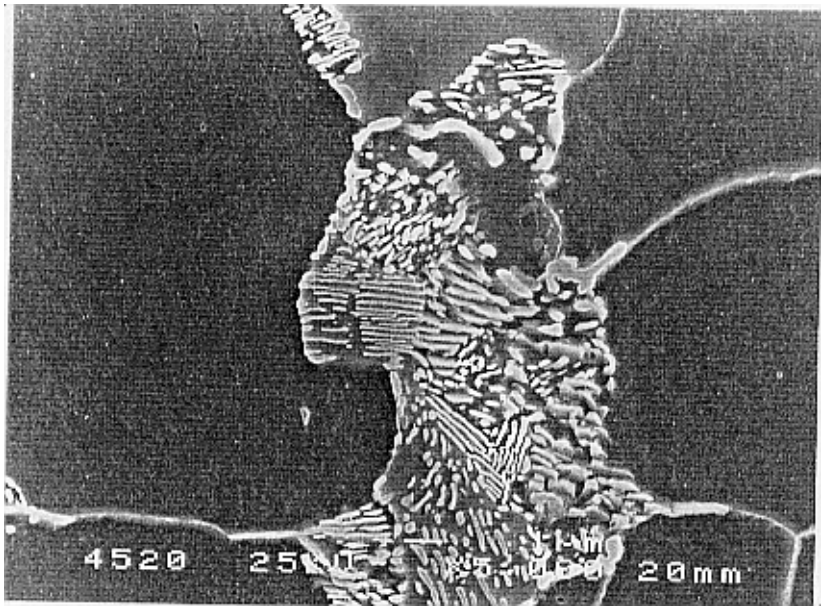

Figs. 3 and 4. Steel St 35.8: 600°C / 3 h, P_{LM} (C = 14) = 12 600, stage A/B. Magnification 1500x (Fig. 3) and 5000x (Fig. 4).

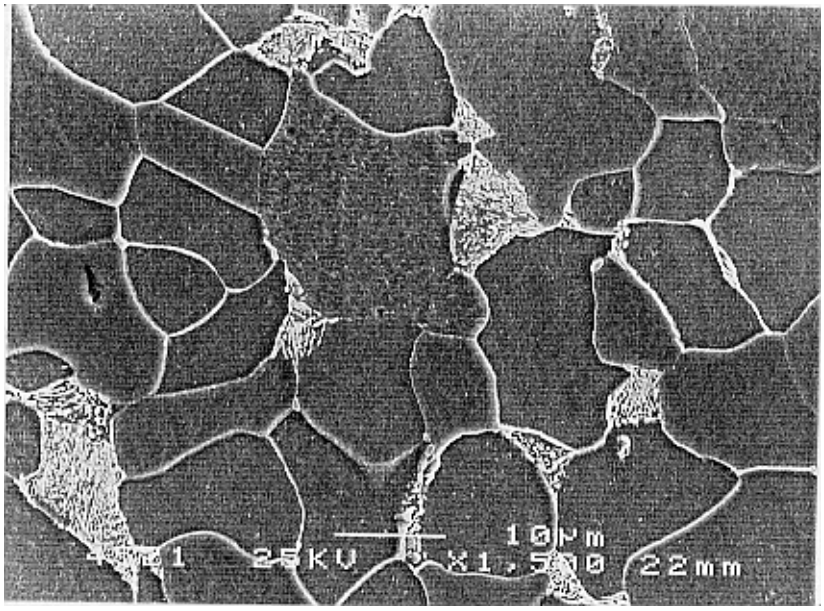

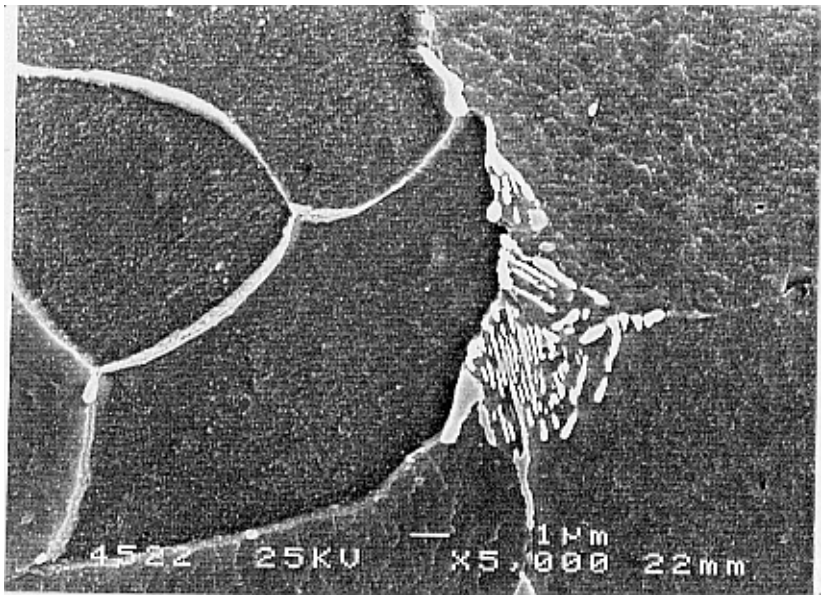

Figs. 5 and 6. Steel St 35.8: 600°C / 10 h, P_{LM} (C = 14) = 13 100, stage B. Magnification 1500x (Fig. 5) and 5000x (Fig. 6).

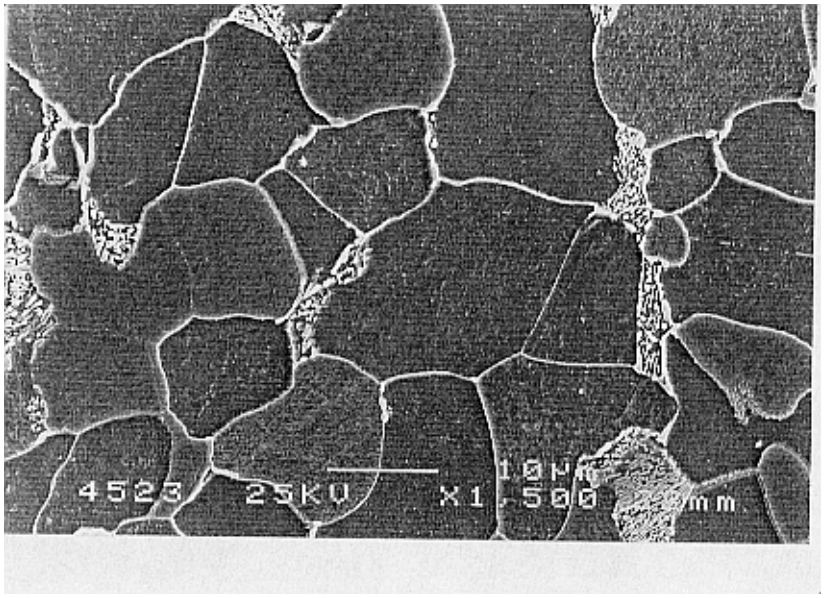

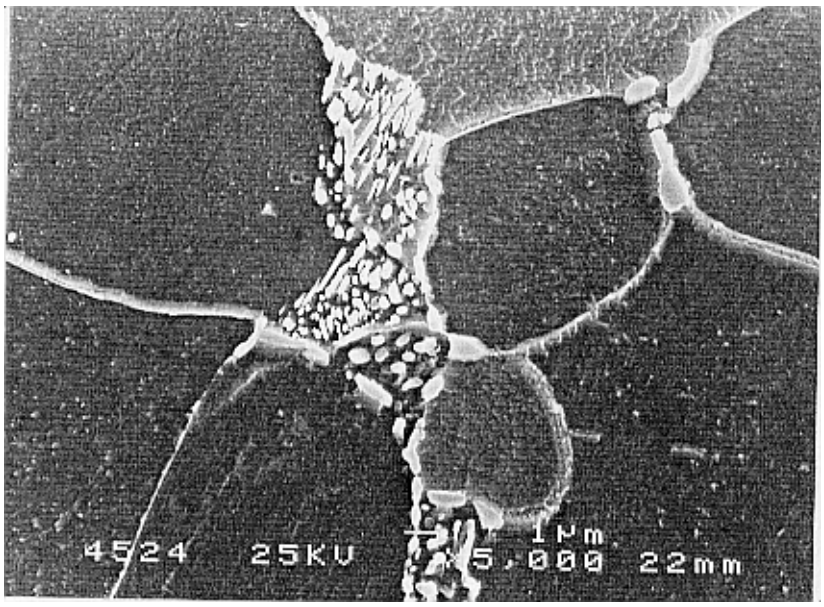

Figs. 7 and 8. Steel St 35.8: 600°C / 30 h, P_{LM} (C = 14) = 13 500, stage C. Magnification 1500x (Fig. 7) and 5000x (Fig. 8).

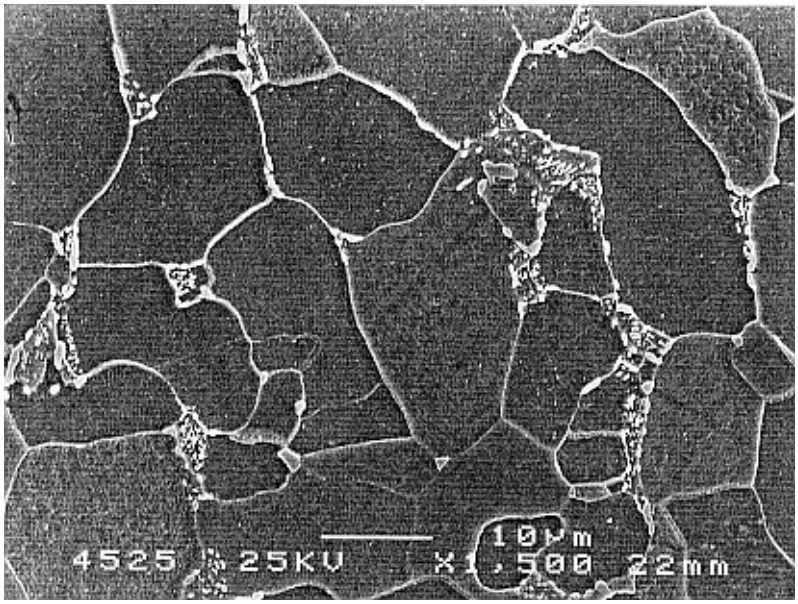

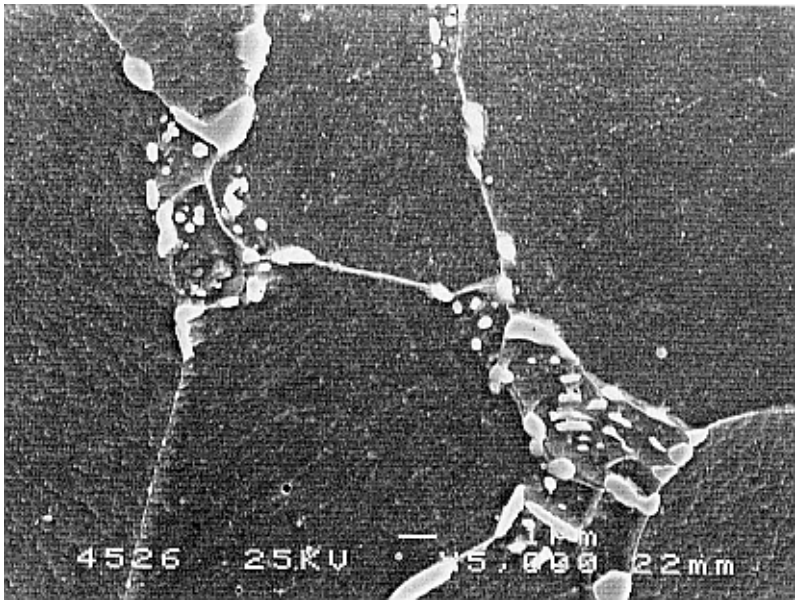

Figs. 9 and 10. Steel St 35.8: 600°C / 100 h, P_{LM} (C = 14) = 14 000, stage D. Magnification 1500x (Fig. 9) and 5000x (Fig. 10).

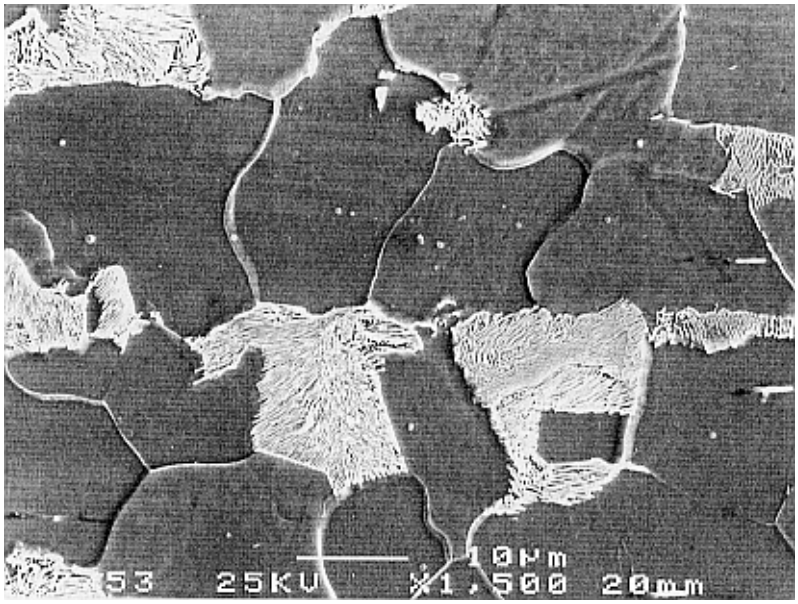

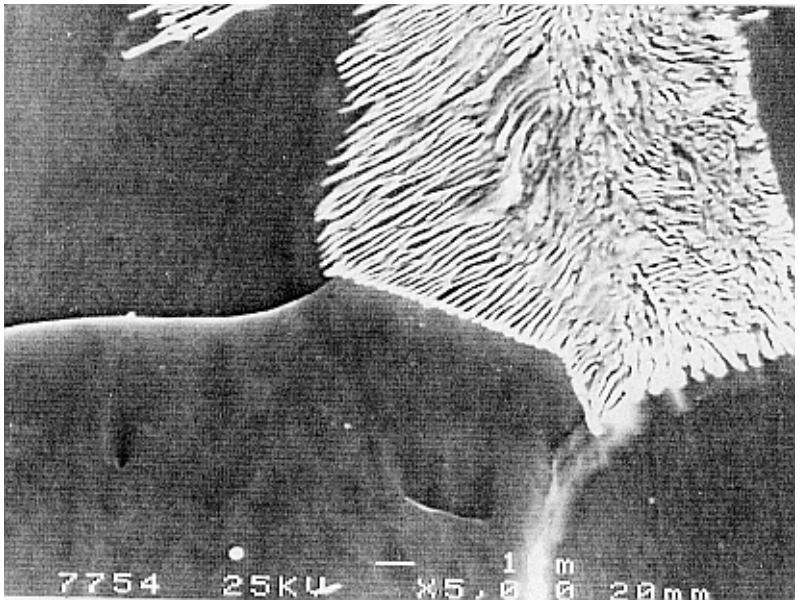

Figs. 11 and 12. Steel 15 Mo 3: as new, stage A. Magnification 1500x (Fig. 11) and 5000x (Fig. 12).

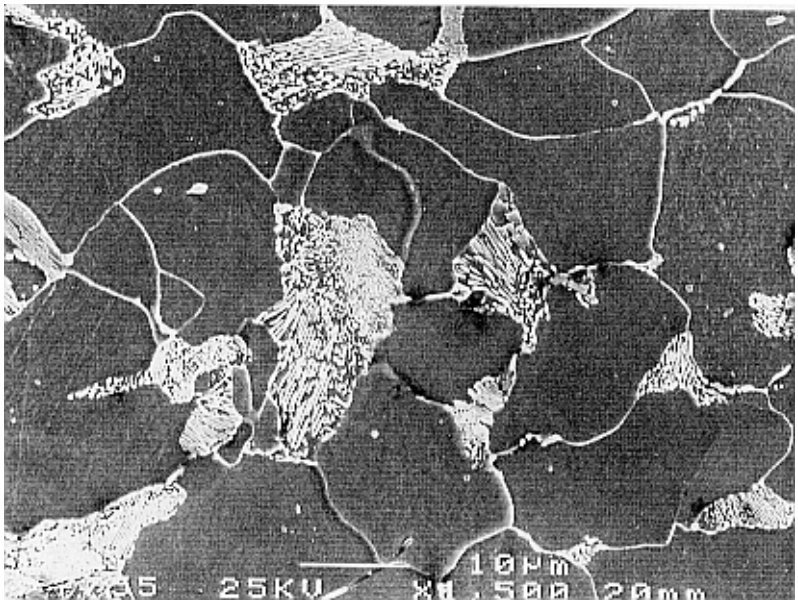

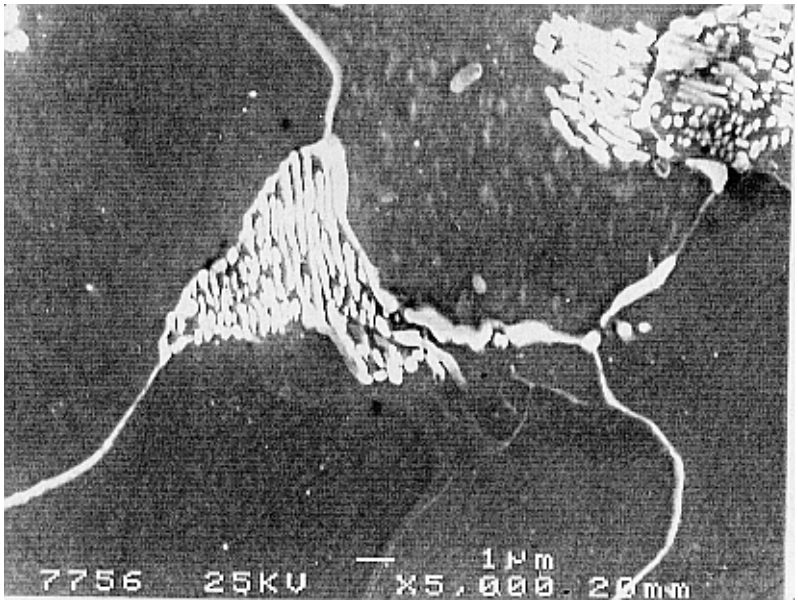

Figs. 13 and 14. Steel 15 Mo 3: 600°C / 10 h, P_{LM} (C = 14) = 13 100, stage A/B. Magnification 1500x (Fig. 13) and 5000x (Fig. 14).

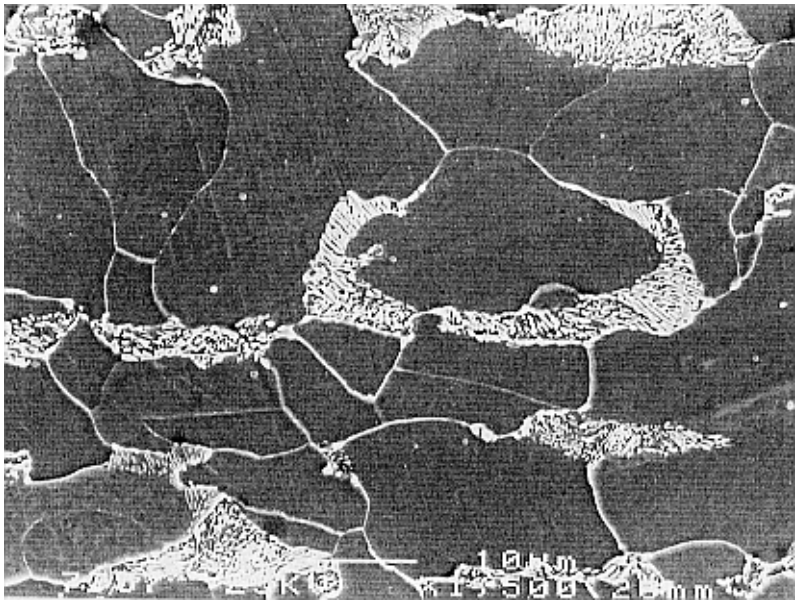

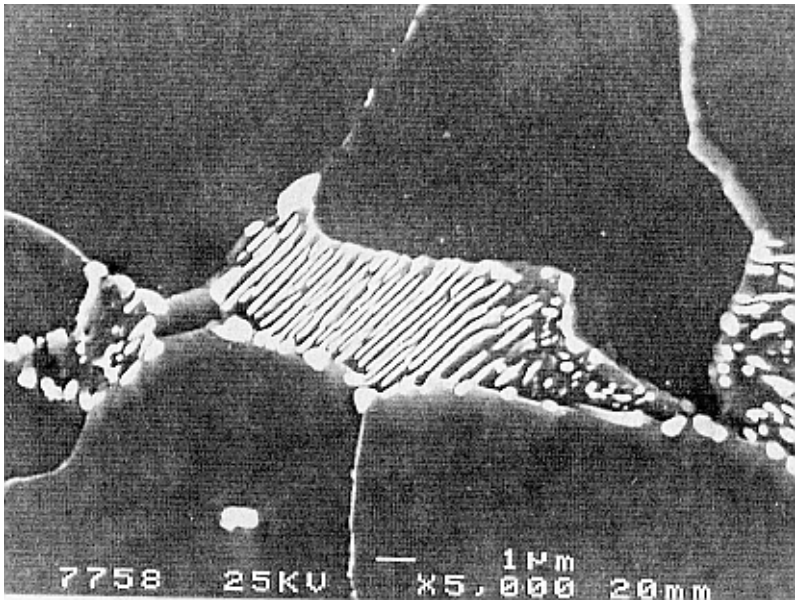

Figs. 15 and 16. Steel 15 Mo 3: 600°C / 30 h, P_{LM} (C = 14) = 13 500, stage B. Magnification 1500x (Fig. 15) and 5000x (Fig. 16).

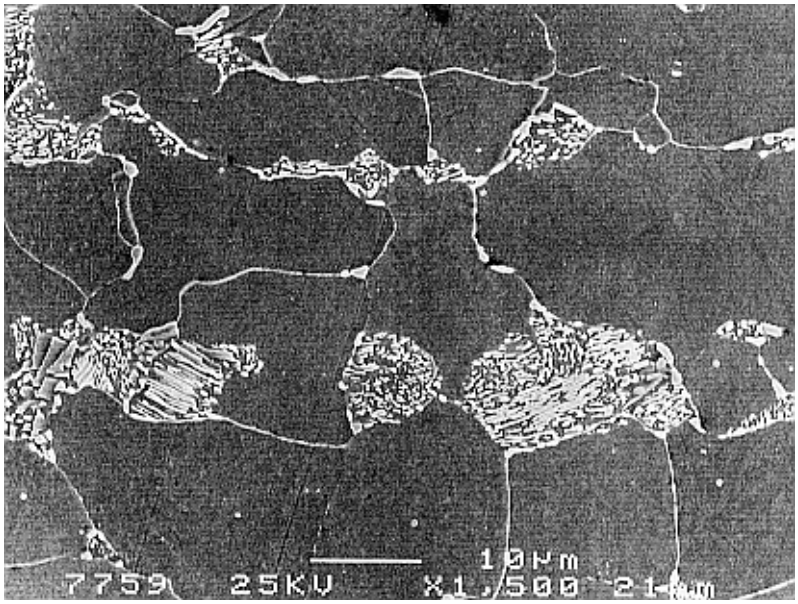

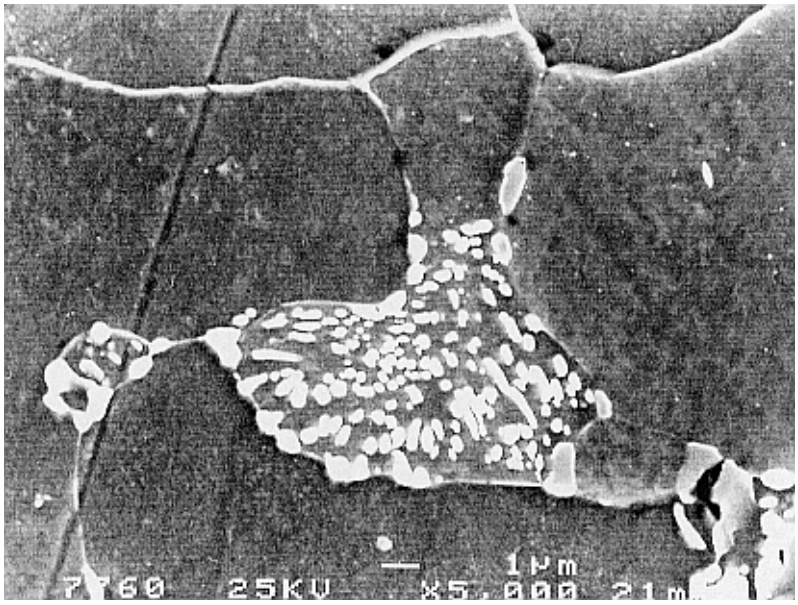

Figs. 17 and 18. Steel 15 Mo 3: 600°C / 100 h, P_{LM} (C = 14) = 14 000, stage C. Magnification 1500x (Fig. 17) and 5000x (Fig. 18).

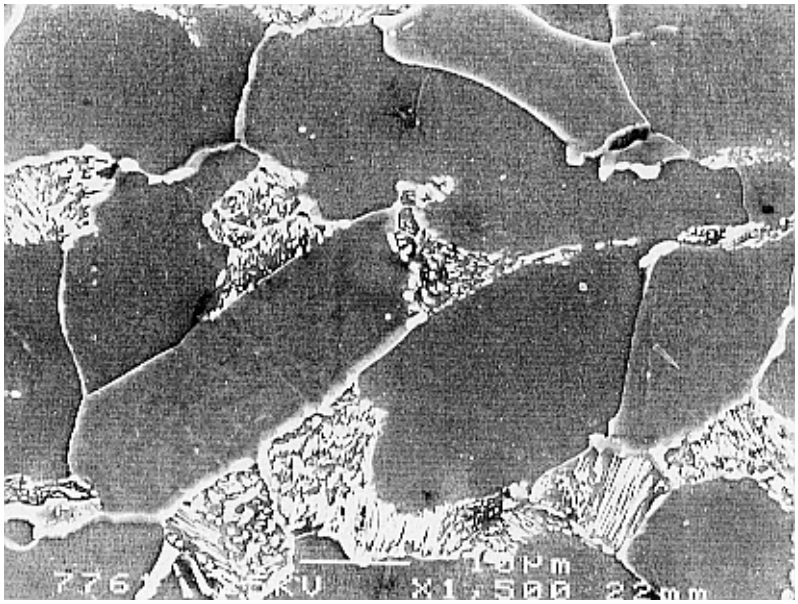

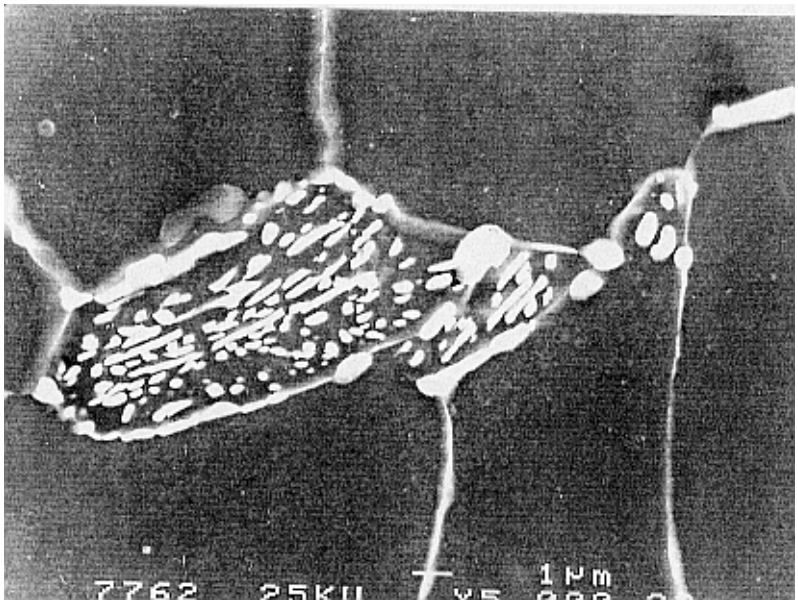

Figs. 19 and 20. Steel 15 Mo 3: 600°C / 300 h, P_{LM} (C = 14) = 14 400, stage D. Magnification 1500x (Fig. 19) and 5000x (Fig. 20).

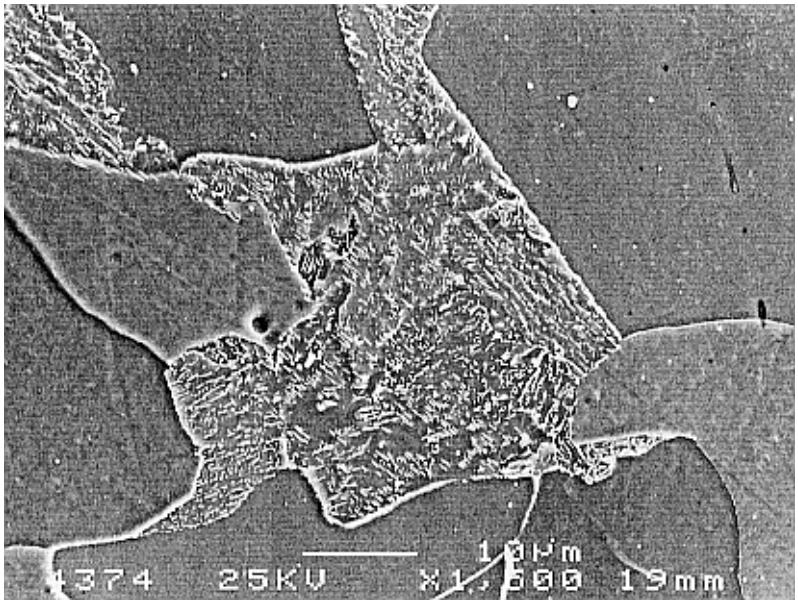

Figs. 21 and 22. Steel 13 CrMo 4 4: as new, stage B. Magnification 1500x (Fig. 21) and 5000x (Fig. 22).

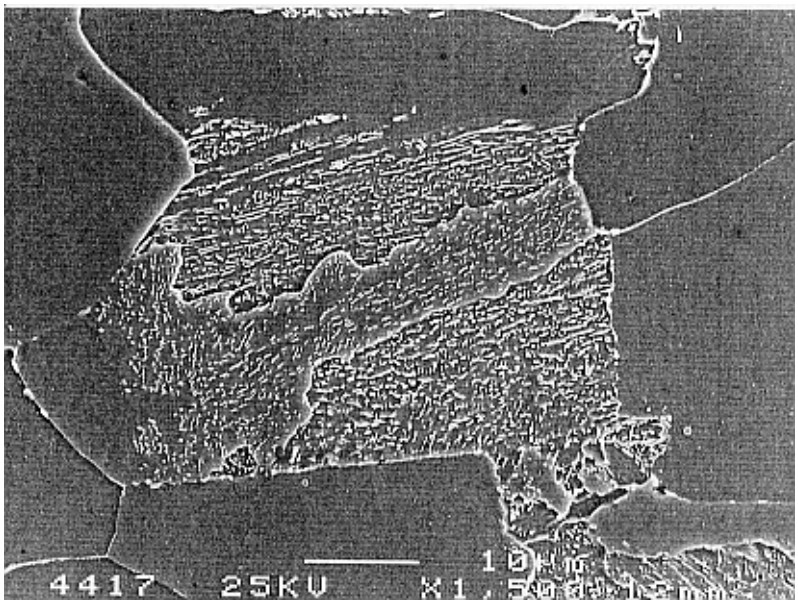

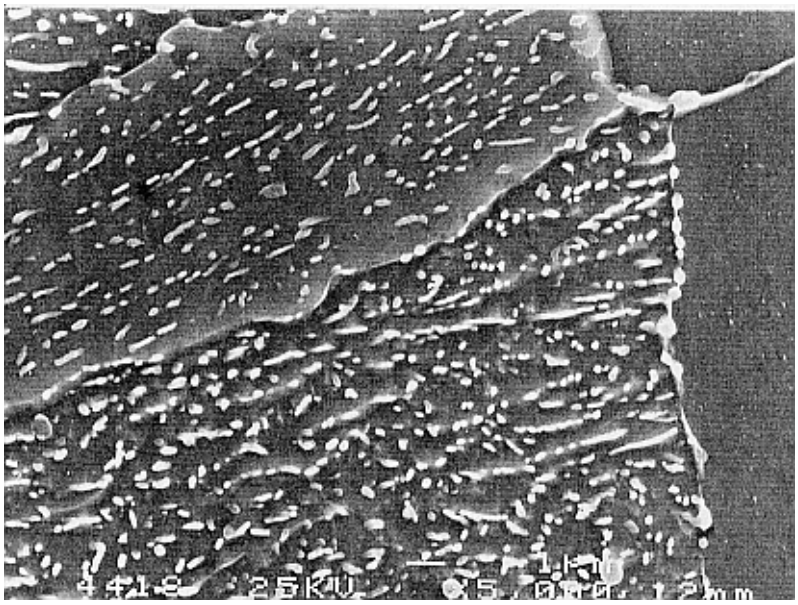

Figs. 23 and 24. Steel 13 CrMo 4 4: 720°C / 3 h, P_{LM} (C = 12) = 12 400, P_{LM} (C = 14) = 14 400, stage B. Magnification 1500x (Fig. 23) and 5000x (Fig. 24).

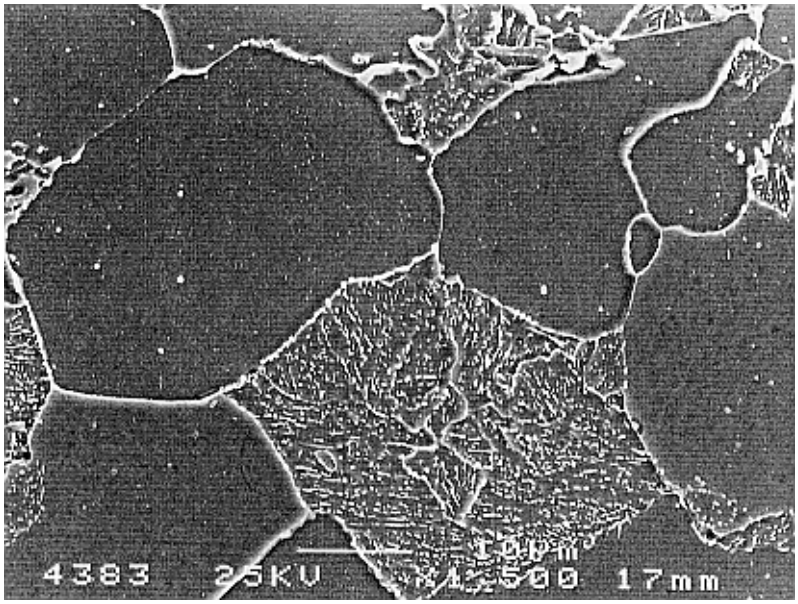

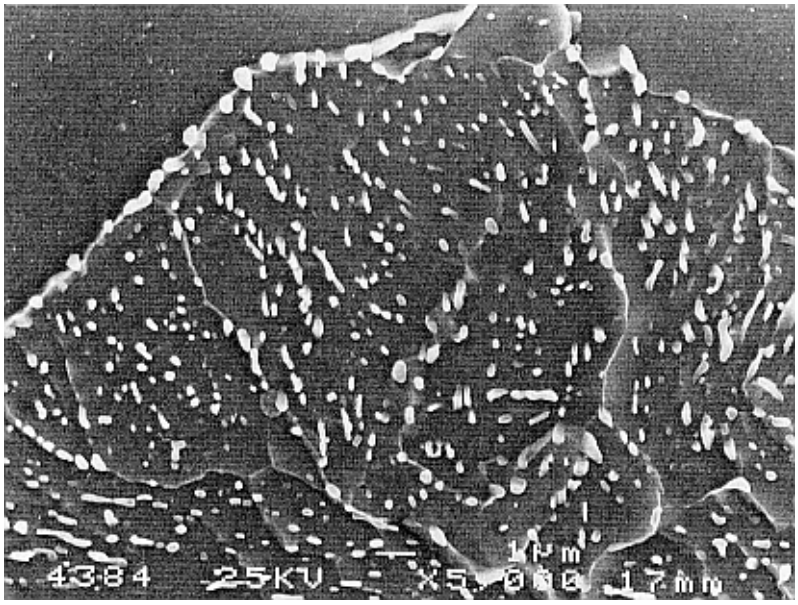

Figs. 25 and 26. Steel 13 CrMo 4 4: 720°C / 10 h, P_{LM} (C = 12) = 12 900, P_{LM} (C = 14) = 14 900, stage C. Magnification 1500x (Fig. 25) and 5000x (Fig. 26).

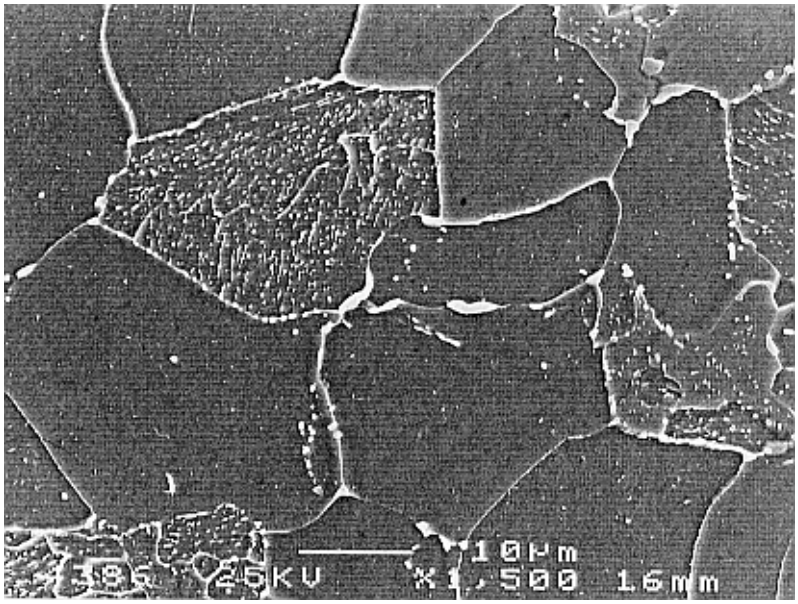

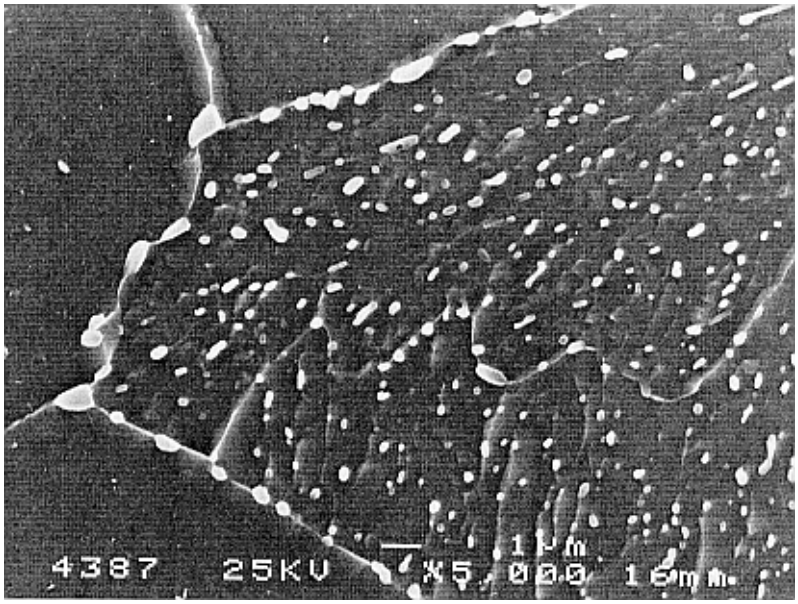

Figs. 27 and 28. Steel 13 CrMo 4 4: 720°C / 30 h, P_{LM} (C = 12) = 13 400, P_{LM} (C = 14) = 15 400, stage D. Magnification 1500x (Fig. 27) and 5000x (Fig. 28).

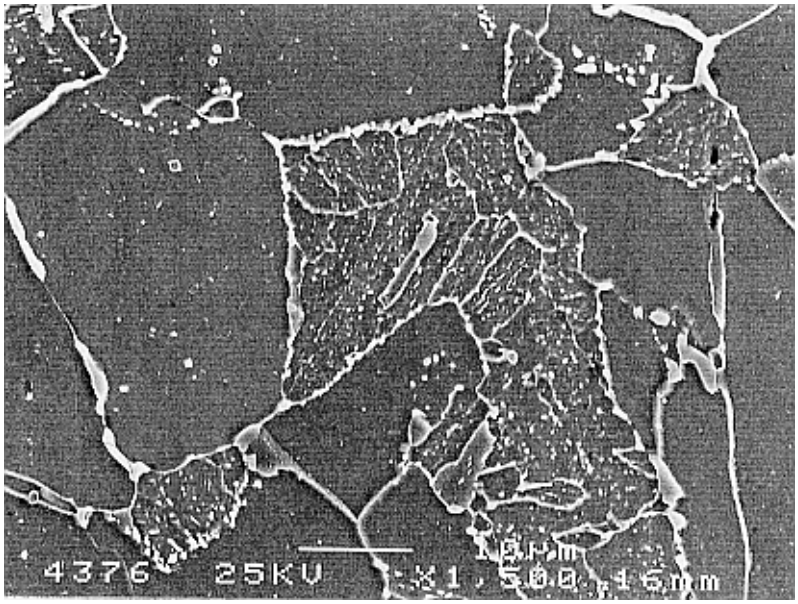

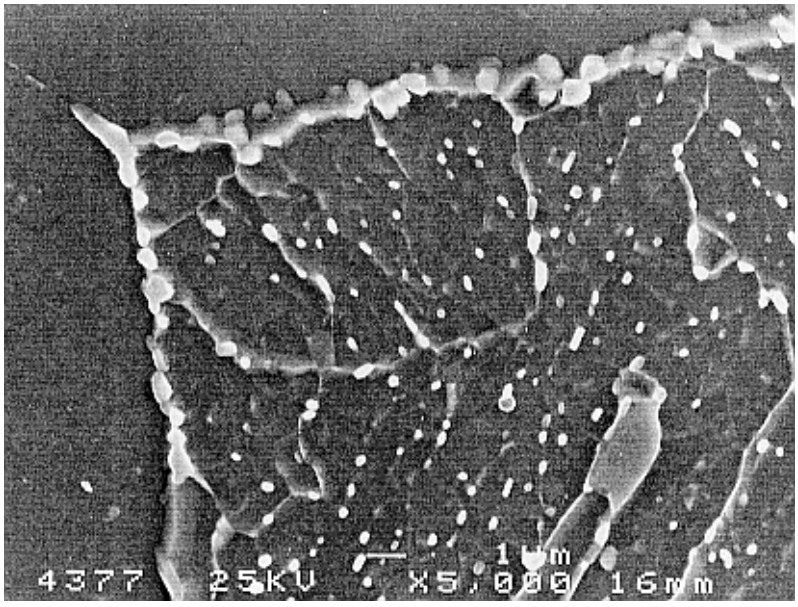

Figs. 29 and 30. Steel 13 CrMo 4 4: 720°C / 100 h, P_{LM} (C = 12) = 13 900, P_{LM} (C = 14) = 15 900, stage E. Magnification 1500x (Fig. 29) and 5000x (Fig. 30).

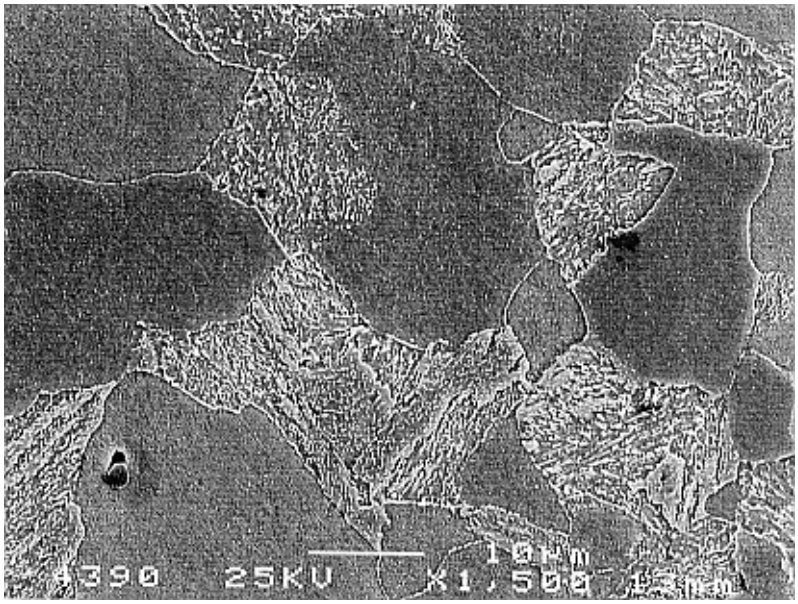

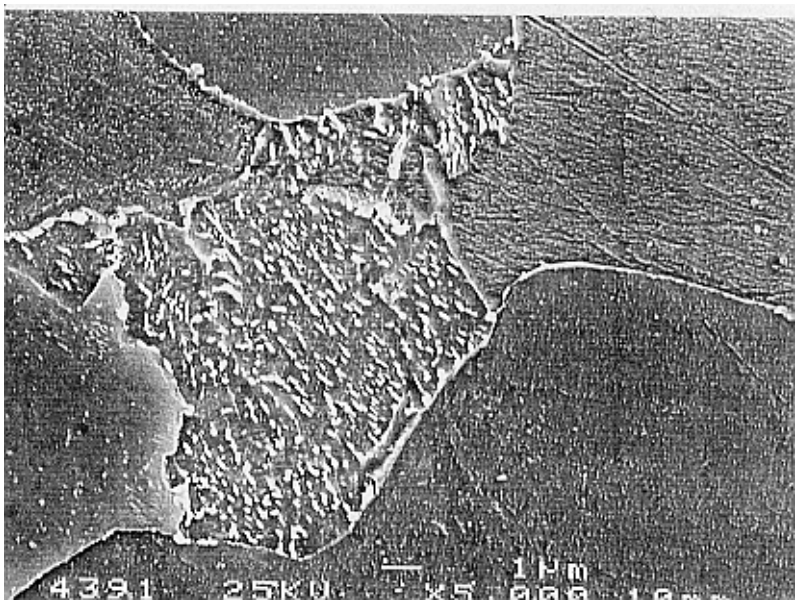

Figs. 31 and 32. Steel 10 CrMo 9 10: as new, stage B. Magnification 1500x (Fig. 31) and 5000x (Fig. 32).

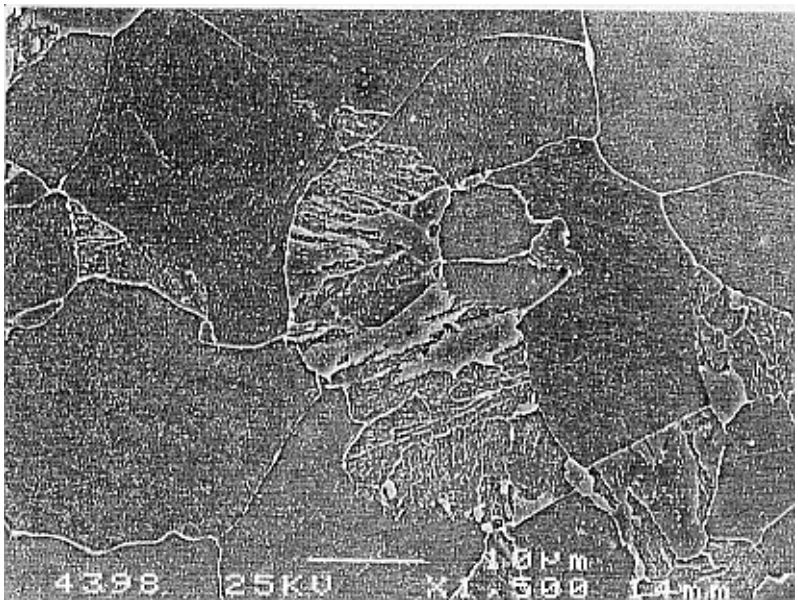

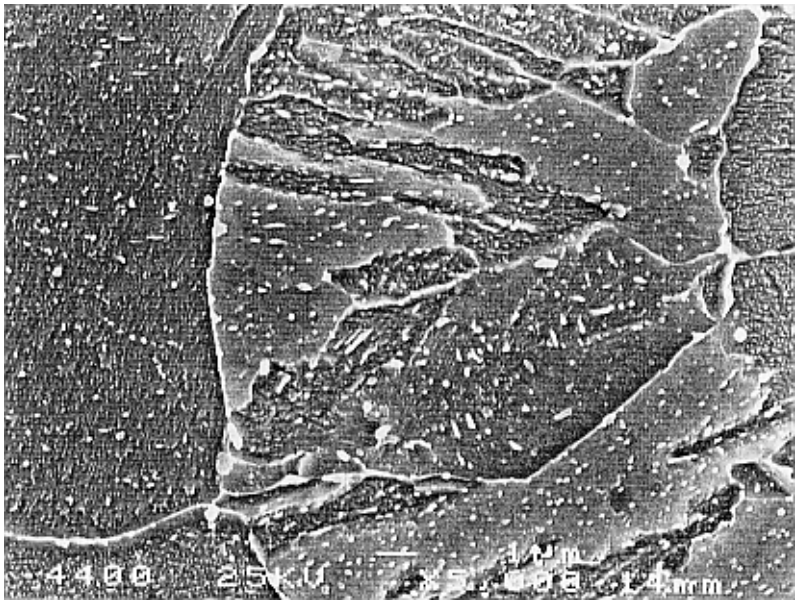

Figs. 33 and 34. Steel 10 CrMo 9 10: 720°C / 3 h, P_{LM} (C = 14) = 14 400, stage B/C. Magnification 1500x (Fig. 33) and 5000x (Fig. 34).

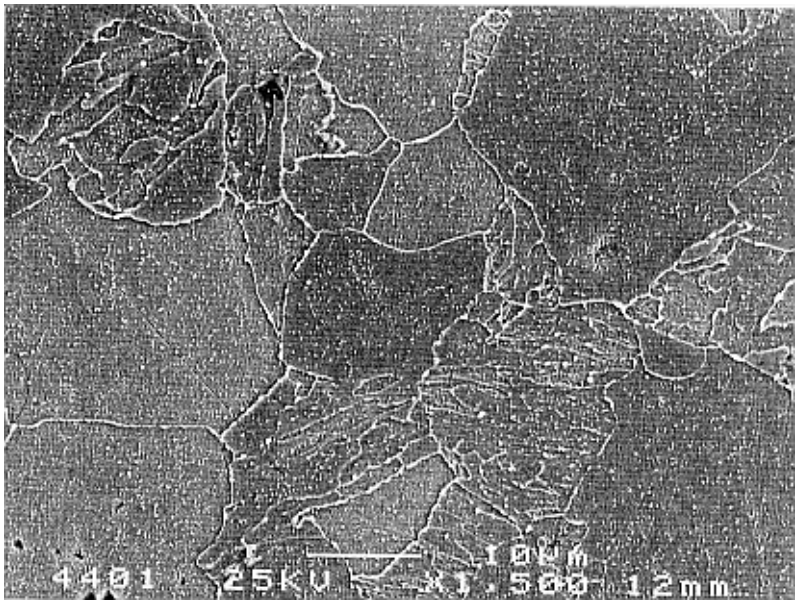

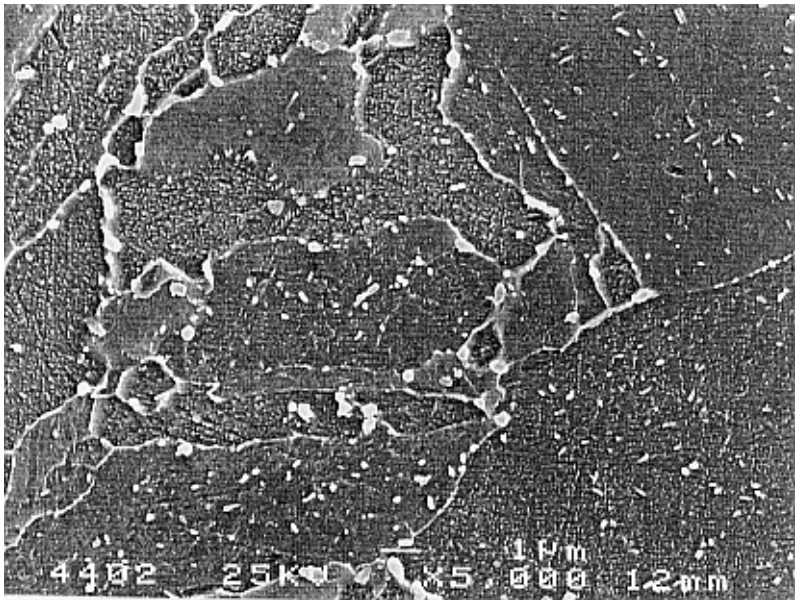

Figs. 35 and 36. Steel 10 CrMo 9 10: 720°C / 10 h, P_{LM} (C = 14) = 14 900, stage C. Magnification 1500x (Fig. 35) and 5000x (Fig. 36).

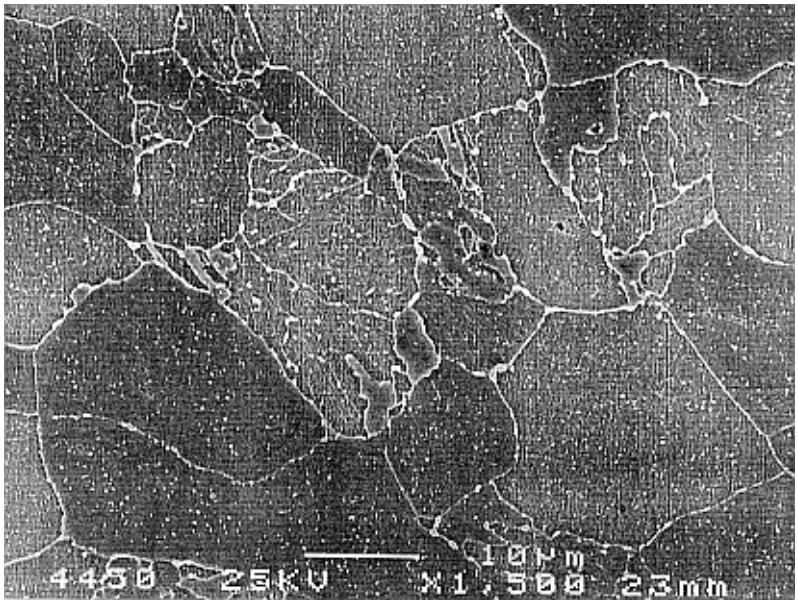

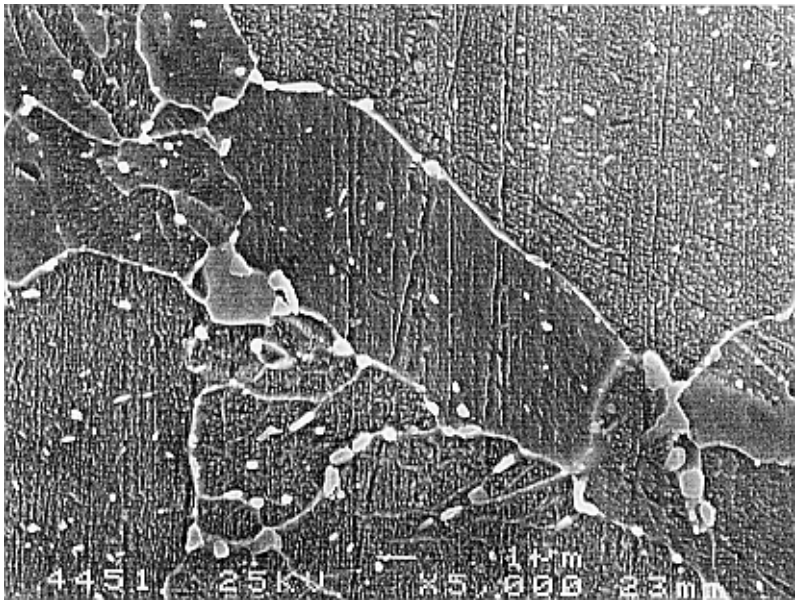

Figs. 37 and 38. Steel 10 CrMo 9 10: 720°C / 30 h, P_{LM} (C = 14) = 15 400, stage D. Magnification 1500x (Fig. 37) and 5000x (Fig. 38).

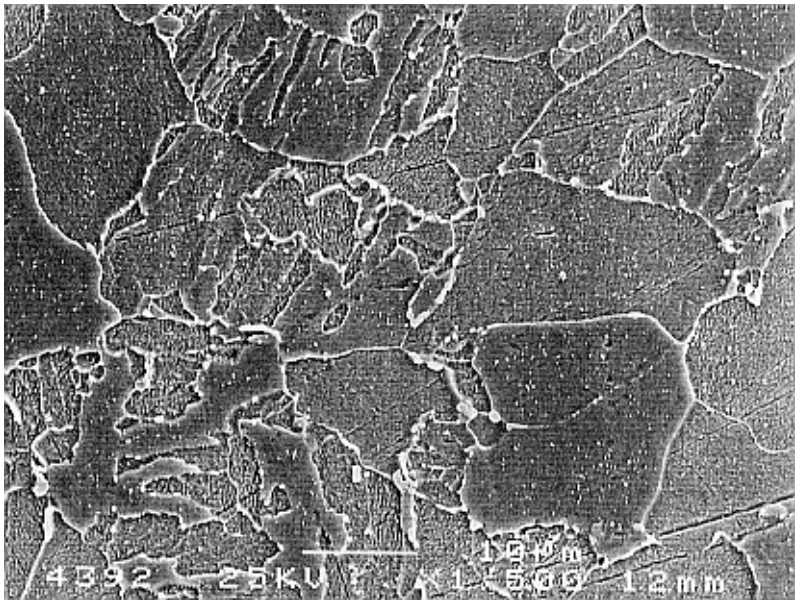

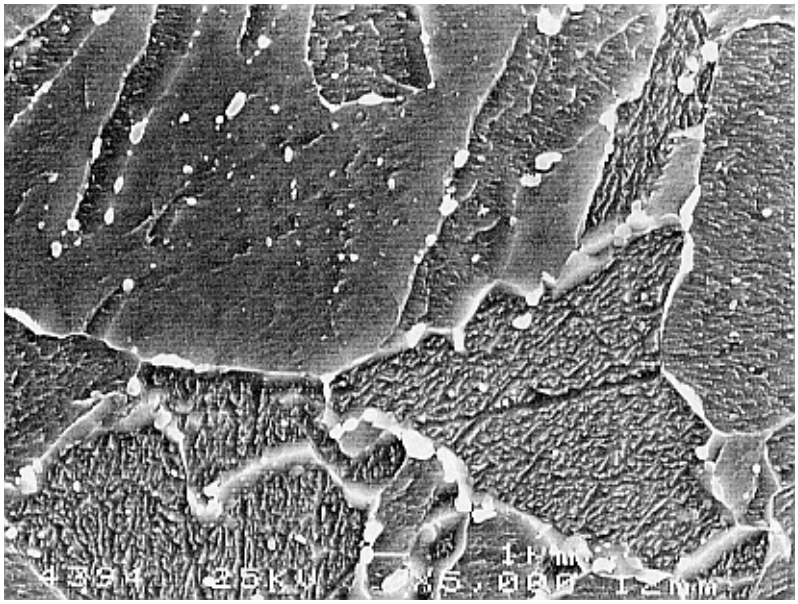

Figs. 39 and 40. Steel 10 CrMo 9 10: 720°C / 100 h, P_{LM} (C = 14) = 15 900, stage D. Magnification 1500x (Fig. 39) and 5000x (Fig. 40).

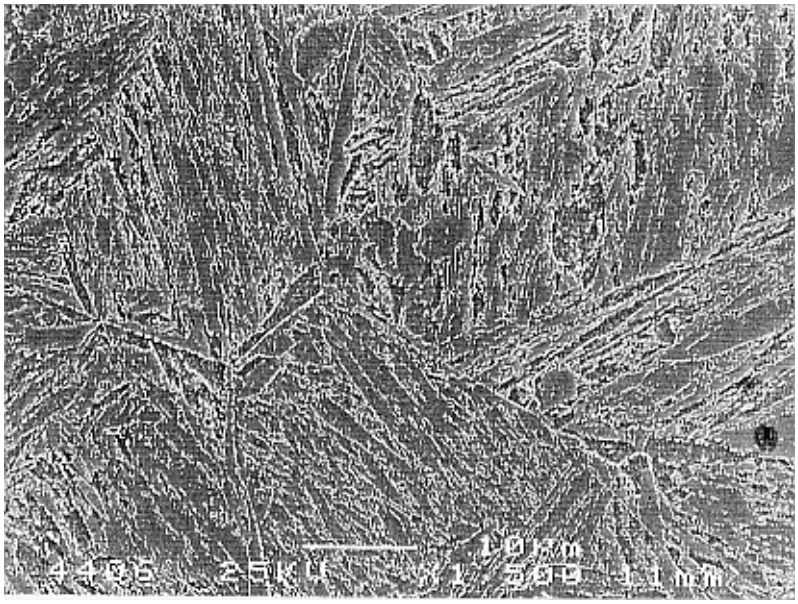

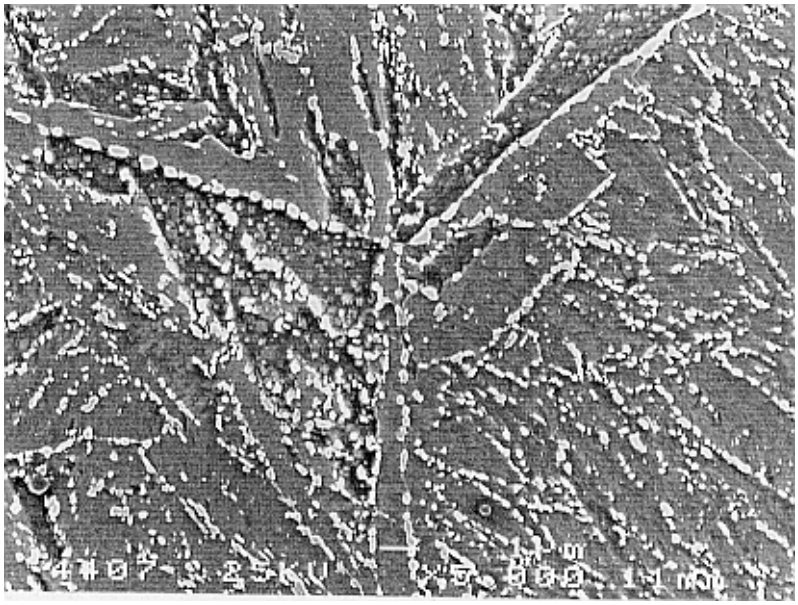

Figs. 41 and 42. Steel X 20 CrMoV 12 1: as new, stage B. Magnification 1500x (Fig. 41) and 5000x (Fig. 42).

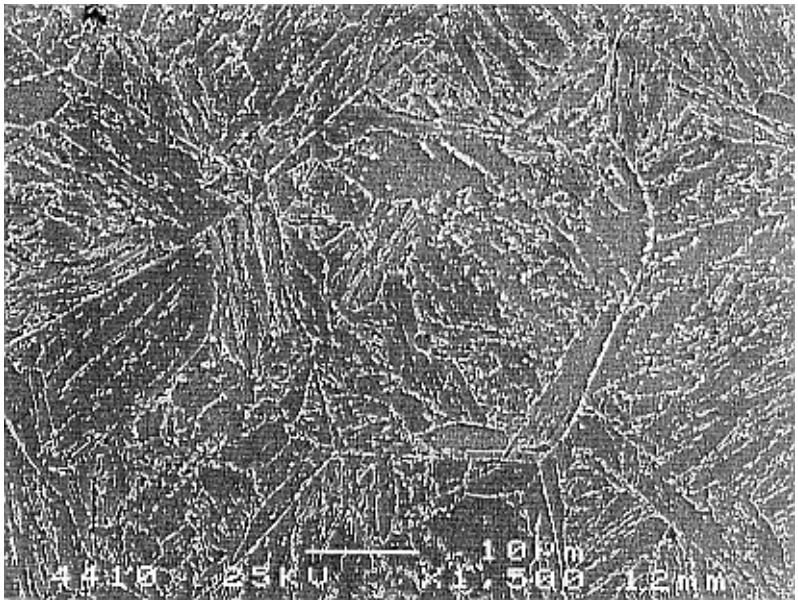

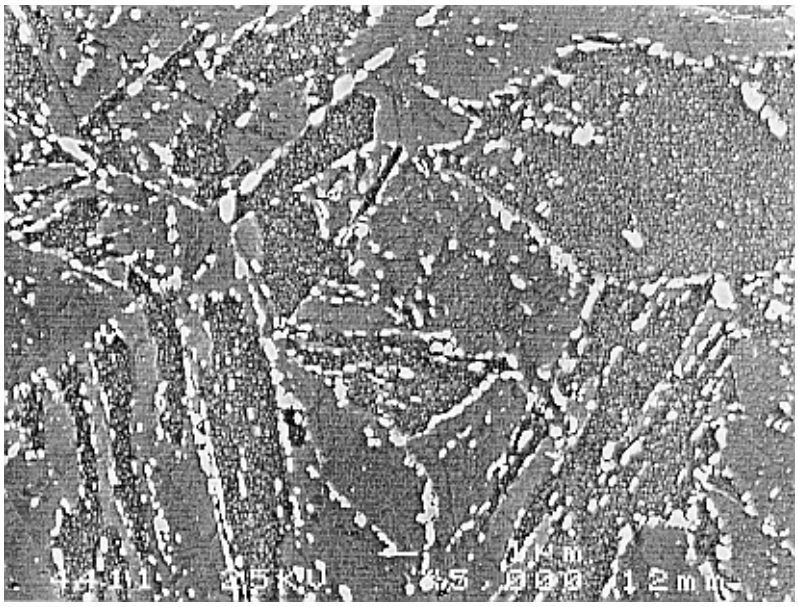

Figs. 43 and 44. Steel X 20 CrMoV 12 1: 780°C / 3 h, P_{LM} (C = 14) = 15 200, stage B/C. Magnification 1500x (Fig. 43) and 5000x (Fig. 44).

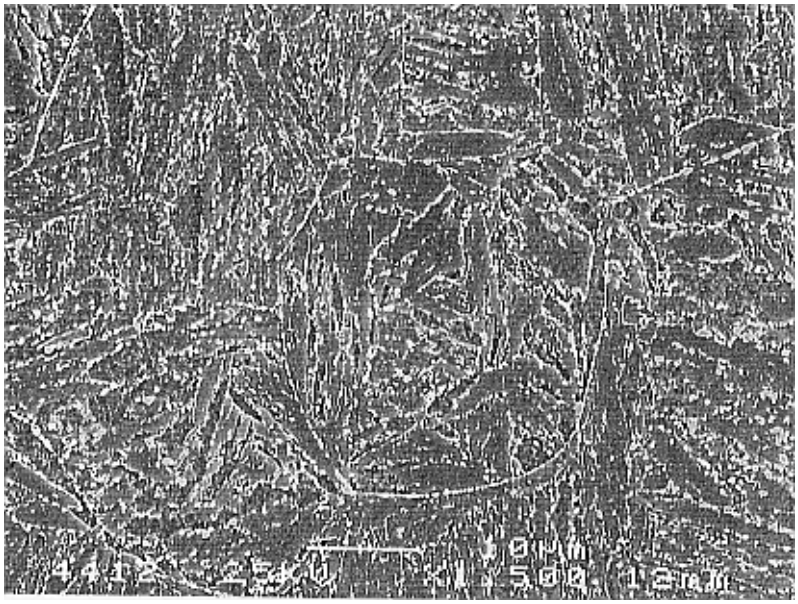

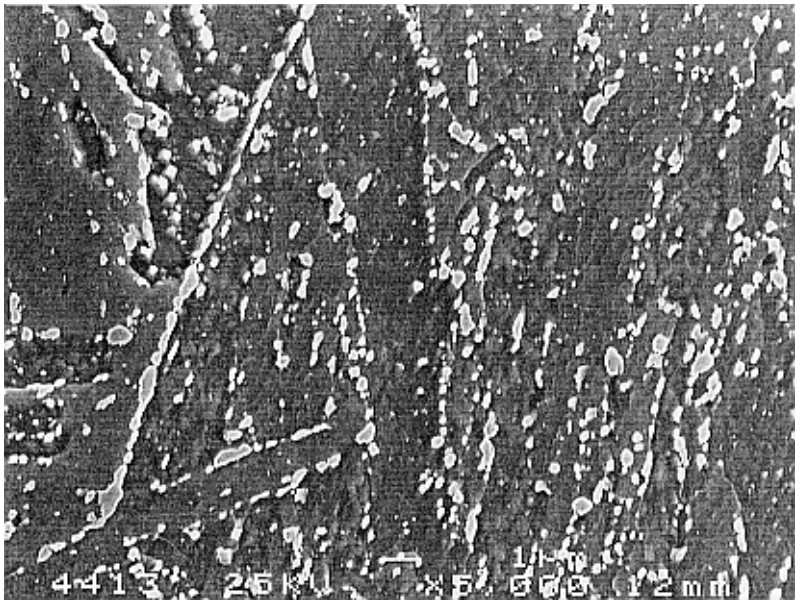

Figs. 45 and 46. Steel X 20 CrMoV 12 1: 780°C / 10 h, P_{LM} (C = 14) = 15 800, stage C. Magnification 1500x (Fig. 45) and 5000x (Fig. 46).

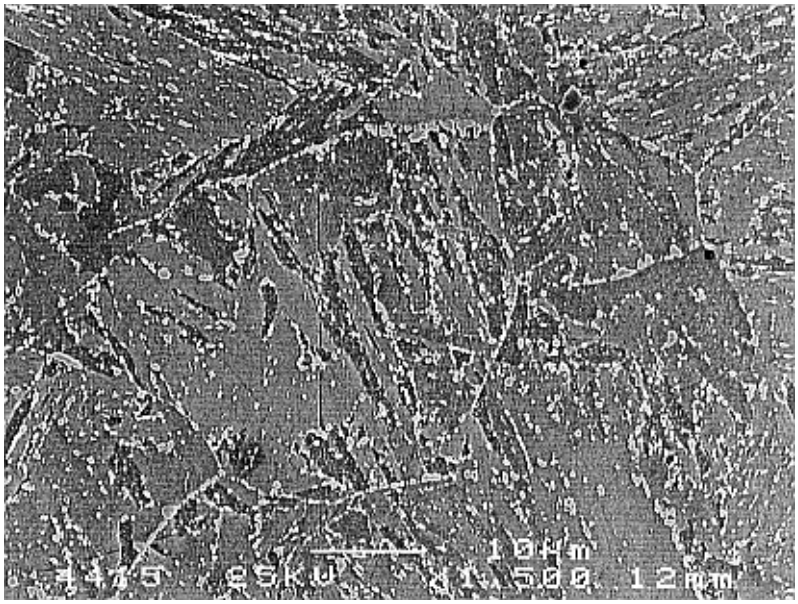

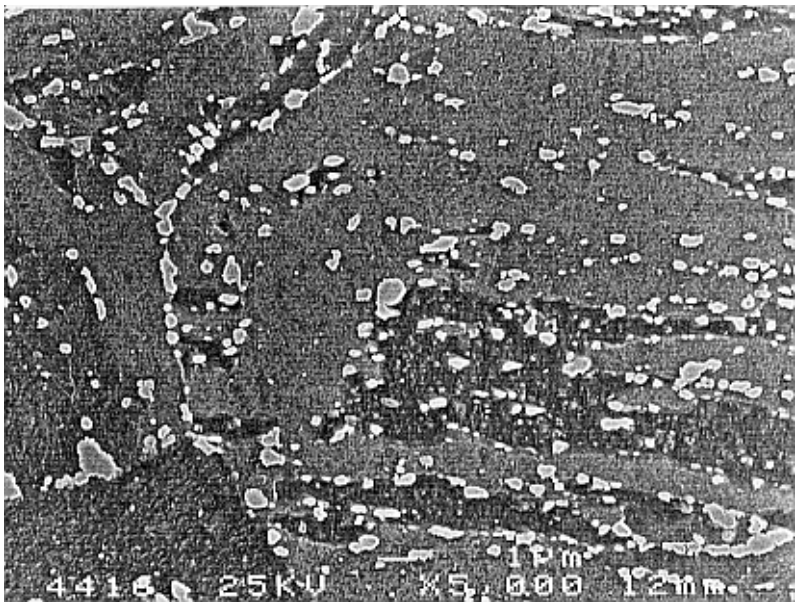

Figs. 47 and 48. Steel X 20 CrMoV 12 1: 780°C / 30 h, P_{LM} (C = 14) = 16 300, stage D. Magnification 1500x (Fig. 47) and 5000x (Fig. 48).

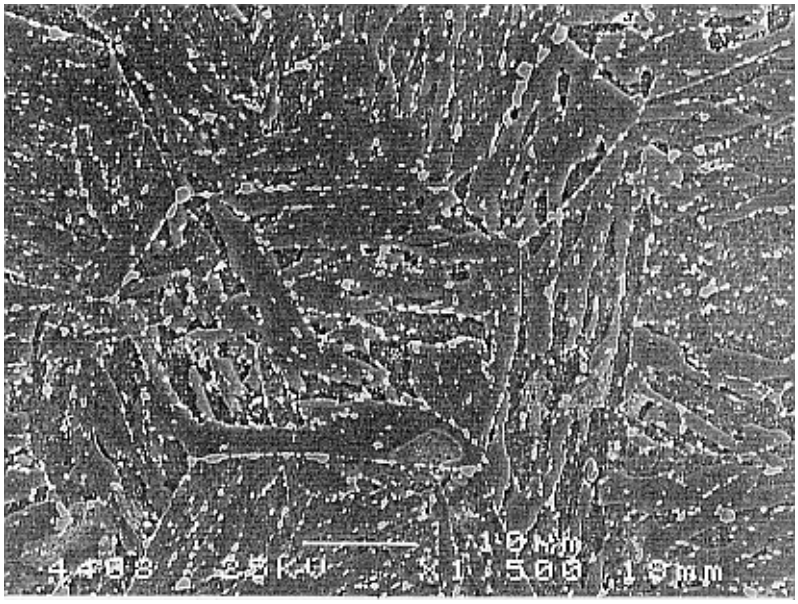

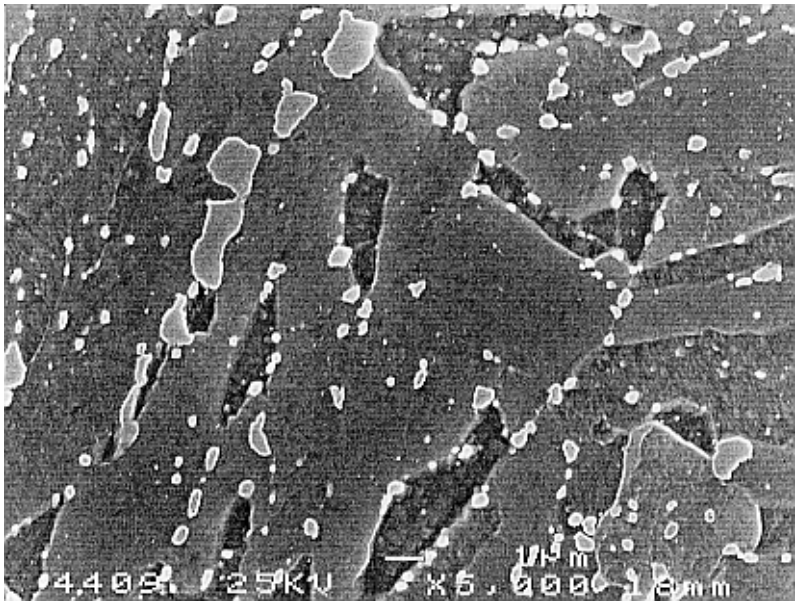

Figs. 49 and 50. Steel X 20 CrMoV 12 1: 780°C / 100 h, P_{LM} (C = 14) = 16 800, stage E. Magnification 1500x (Fig. 49) and 5000x (Fig. 50).